

System Identification and Control Using Lyapunov-Based Deep Neural Networks without Persistent Excitation: A Concurrent Learning Approach

Rebecca G. Hart, Omkar Sudhir Patil, Zachary I. Bell, and Warren E. Dixon

Abstract—Deep Neural Networks (DNNs) are increasingly used in control applications due to their powerful function approximation capabilities. However, many existing formulations focus primarily on tracking error convergence, often neglecting the challenge of identifying the system dynamics using the DNN. This paper presents the first result on simultaneous trajectory tracking and online system identification using a DNN-based controller, without requiring persistent excitation. Two new concurrent learning adaptation laws are constructed for the weights of all the layers of the DNN, achieving convergence of the DNN’s parameter estimates to a neighborhood of their ideal values, provided the DNN’s Jacobian satisfies a finite-time excitation condition. A Lyapunov-based stability analysis is conducted to ensure convergence of the tracking error, weight estimation errors, and observer errors to a neighborhood of the origin. Simulations performed on a range of systems and trajectories, with the same initial and operating conditions, demonstrated 40.5% to 73.6% improvement in function approximation performance compared to the baseline, while maintaining a similar tracking error and control effort. Simulations evaluating function approximation capabilities on data points outside of the trajectory resulted in 58.88% and 74.75% improvement in function approximation compared to the baseline.

I. INTRODUCTION

Deep Neural Networks (DNNs) have become increasingly popular due to their powerful function approximation capabilities [1]–[13]. However, typical DNN-based estimators use offline optimization methods to train the network weights. Such approaches require large data sets and do not provide online persistent learning of unknown dynamics which is relevant in applications which experience changes in the underlying dynamics over time such as those involving smart materials, fluid structure interaction, or human-machine interactions. Motivated by these issues, [1] and [2] introduced a DNN-based architecture which allows the outer

This research is supported in part by the National Science Foundation Graduate Research Fellowship under Grant No. DGE-2236414, AFRL grant FA8651-24-1-0018, and AFOSR grant FA9550-19-1-0169. Any opinions, findings, and conclusions or recommendations expressed in this material are those of the author(s) and do not necessarily reflect the views of the sponsoring agency.

Rebecca G. Hart, Omkar Sudhir Patil, and Warren E. Dixon are with the Department of Mechanical and Aerospace Engineering, University of Florida, Gainesville, FL 32611 Emails: {rebecca.hart, patilomkarsudhir, wdixon}@ufl.edu.

Zachary I. Bell is with the Munitions Directorate, Air Force Research Laboratory, Eglin AFB, FL 32542 Email: zachary.bell.10@us.af.mil

layer weights to adapt in real time while the inner layer weights are held static with periodic updates using offline training techniques. Recent advancements in results such as [3], [7], [8], [14]–[18] (termed Lyapunov-based (Lb)-DNNs) have enabled online weight adaptation for all the weights in a DNN, demonstrating improved tracking performance over shallow NN approaches or traditional offline training methods. However, these approaches have primarily focused on tracking objectives and not parameter convergence or system identification. System identification is an important objective because it allows the identified model to provide insights that could be used in a variety of applications, such as fault detection, or the ability to predict accurate state estimates during intermittent loss of state feedback [19].

For systems involving linear-in-parameter (LIP) uncertainty, results such as [20], [21] and [22]–[24] have developed methods to achieve parameter convergence without requiring persistent excitation (PE), by incorporating data from previously explored trajectories into the parameter update laws. The approach in [6] used a LIP representation of a DNN by allowing the output layer weights to adapt in real time and held the inner layer weights static and applied the standard concurrent learning (CL) method on the output layer weights. CL techniques, construct a history stack of past information, resulting in improved system identification as well as enabling off-trajectory exploration [22], [23]. This capability reduces over-reliance on instantaneous observations and includes a wider range of past observations in the update process, reducing the risk of converging to local minima. However, the nonlinear-in parameter (NIP) structure of a DNN’s inner layer presents challenges in extending the CL update to all layers of the DNN making it an open problem.

The system identification objective is difficult to achieve using DNNs because they have nested nonlinearities and a NIP structure. While classical adaptive control methods are known to achieve parameter convergence for LIP uncertainties under the persistence of excitation (PE) condition, only a few works consider NIP uncertainties [4]–[6], [20], [21], [25]. The result in [26] considers convex/concave nonlinear parameterizations to achieve global convergence of parameter estimates, and the results in [27] and [28] consider strongly monotonic nonlinear parameterizations. However, the NIP structure of DNNs is neither convex/concave nor strongly

monotonic.

Motivated by the desire to achieve parameter convergence, results such as [4]–[6], [20], [21], [25] use adaptive control techniques to yield convergence of parameter estimates to a neighborhood of the actual parameters. In [4] and [5], a prediction error formulation was constructed using a dynamic state derivative estimator and a least squares update law based on the DNN’s Jacobian. This approach resulted in parameter estimation error convergence to a neighborhood of the origin, provided the Jacobian of the DNN satisfies the PE condition. However, the PE condition on the Jacobian cannot be verified online for nonlinear systems and requires continuous exploration of system states and parameter trajectories; hence, posing a challenge in balancing exploration and exploitation. Thus, online system identification for DNNs without the PE condition remains an open problem.

This work presents the first approach for continuous all-layer adaptation of a DNN informed by historical performance, using a CL-based update law (hereafter referred to as Lb-CL-DNN). The use of the CL-based update law relaxes the PE condition which is typical in other results and yields convergence of the parameter estimates to a neighborhood of the actual parameters under finite excitation (FE). Section II provides generalized identifiability conditions for nonlinear regression equations (NREs) which are applicable to NIP models and demonstrates that the FE condition is equivalent to ensuring that the unknown parameters are identifiable. To overcome the challenges associated with the NIP structure of the DNN, a first-order Taylor series approximation is strategically applied at various recorded data-points. Then, two different formulations are provided to construct a history stack using the DNN’s Jacobian and the Taylor series approximation applied on the data-points. Section II demonstrates the update law on a continuous time regression problem and provides a Lyapunov-based stability analysis to show the convergence of the weight estimation errors. Sections III–V apply the developed CL method to the adaptive control problem which involves additional complexities due to the resulting regression involving state-derivative terms which are typically noisy or unavailable. Therefore, a dynamic state-derivative estimator is developed with a prescribable settling time guarantee. By only collecting data after the prescribed settling time, we prevent transient state estimation errors from corrupting the history stack. Eliminating such transient errors is important in this result because, unlike LIP regressions, the DNN’s Jacobian depends on the parameter estimates, and transient errors would result in the history stack being filled with inaccurate estimates. To address inaccuracies, two update laws were developed, each dynamically reconstructing the history stack with newer parameter estimates and leveraging distinct properties of DNNs to ensure accurate parameter estimation. A Lyapunov-based stability analysis guarantees boundedness of the tracking error, weight estimation errors, and observer errors. Simulations on multiple systems and trajectories under the same operating conditions demonstrated a 40.5% to 73.6% improvement in system identification compared to the baseline, while maintaining

a similar tracking error and control effort. The improvement in function approximation capabilities was also seen in simulations performed on off-trajectory data, with improvements ranging from 58.88% to 74.75% .

Notation and Mathematical Background

The space of essentially bounded Lebesgue measurable functions is denoted by \mathcal{L}_∞ . Given $A \triangleq [a_{j,i}] \in \mathbb{R}^{n \times m}$, $\text{vec}(A) \triangleq [a_{1,1}, \dots, a_{n,1}, \dots, a_{1,m}, \dots, a_{n,m}]^\top$. The Kronecker product is denoted by \otimes . Given any $A \in \mathbb{R}^{n \times m}$, $B \in \mathbb{R}^{m \times p}$, and $C \in \mathbb{R}^{p \times r}$, $\text{vec}(ABC) = (C^\top \otimes A) \text{vec}(B)$. The right-to-left matrix product operator is represented by $\widehat{\prod}$, i.e., $\prod_{p=1}^m A_p = A_m \dots A_2 A_1$ and $\prod_{p=a}^m A_p = 1$, if $a > m$. The identity matrix of size $n \times n$ is denoted by I_n . The zero vector of size $q \times 1$ is given by 0_q . Given some functions f and g function composition is denoted by \circ , where $(f \circ g)(x) \triangleq f(g(x))$.

A. Deep Neural Network (DNN) Model

DNNs are motivated given the prevalent evidence that indicates their improved function approximation capabilities when compared to shallow NNs [29]. A feedforward DNN $\Phi(X, \theta) \in \mathbb{R}^{L_{k+1}}$ can be modeled as [3]

$$\Phi(X, \theta) \triangleq (v_k^\top \phi_k \circ \dots \circ v_0^\top \phi_1)(v_0^\top X_a), \quad (1)$$

where $\theta \triangleq [\text{vec}(v_0)^\top, \dots, \text{vec}(v_k)^\top]^\top \in \mathbb{R}^\rho$, where $\rho \triangleq \sum_{j=0}^k L_j L_{j+1}$, $j \in \{0, \dots, k\}$ and $k \in \mathbb{N}$ denotes the number of hidden layers within θ , $v_j \in \mathbb{R}^{L_j \times L_{j+1}}$ denotes the matrix of weights and biases in the j^{th} hidden layer, $L_j \in \mathbb{N}$ denotes the number of nodes within the j^{th} hidden layer for all $j \in \{0, \dots, k\}$, $k \in \mathbb{N}$ denotes the number of hidden layers, and $L_0 \triangleq m + 1$, where m is the dimension of the \mathbb{R}^m input vector to the DNN. Where $X \in \Omega$ denotes the input to the DNN, $\Omega \subset \mathbb{R}^m$ denotes a compact set, and the augmented input $X_a \in \mathbb{R}^{m+1}$ is defined as $X_a \triangleq [X^\top \ 1]^\top$. The vector of smooth activation functions at the j^{th} layer is denoted by $\phi_j \in \mathbb{R}^{L_j}$ and is defined as $\phi_j \triangleq [\varsigma_{j,1} \ \dots \ \varsigma_{j,L_j-1} \ 1]^\top$, where $\varsigma_{j,y} \in \mathbb{R}$ denotes the activation function at the y^{th} node of the j^{th} layer for all $j \in \{1, \dots, k\}$. To incorporate a bias term into the DNN model in (1), the input X and the activation functions ϕ_j are augmented with a 1 for all $j \in \{1, \dots, k\}$.

To facilitate the development of the online weight adaptation laws, the DNN model in (1) can also be represented recursively using the shorthand notation Φ_j as [3]

$$\Phi_j \triangleq \begin{cases} v_j^\top \phi_j(\Phi_{j-1}), & j \in \{1, \dots, k\}, \\ v_0^\top X_a & j = 0, \end{cases} \quad (2)$$

where $\Phi(X, \theta) = \Phi_k$.

The Jacobian of the feedforward DNN,¹ denoted $\Phi'(X, \theta)$, can be represented as $\Phi'(X, \theta) \triangleq$

¹A fully-connected DNN model is considered for ease of exposition. However, the CL update laws developed subsequently are agnostic to the DNN architecture and can be applied to other architectures such as [8], [30] based on their Jacobian derivation.

$[\Phi'_0(X, \theta), \dots, \Phi'_j(X, \theta)] \in \mathbb{R}^{n \times \rho}$, where $\Phi'_j \triangleq \frac{\partial \Phi_j(X, \theta)}{\partial \theta} \in \mathbb{R}^{n \times L_{j+1}}$, for all $j \in \{0, \dots, k\}$. Using (2), the chain rule, and properties of the vectorization operator, the terms Φ'_0 and Φ'_j can be expressed as [3]

$$\Phi'_0(X, \hat{\theta}) \triangleq \left(\prod_{l=1}^k v_l^\top \phi'_l \right) \left(I_{L_1} \otimes X_a^\top \right),$$

$$\Phi'_j(X, \theta) \triangleq \left(\prod_{l=j+1}^k v_l^\top \phi'_l \right) \left(I_{L_{j+1}} \otimes \phi_j^\top \right),$$

for all $j \in \{1, \dots, k\}$, where the activation function at the j^{th} layer and its Jacobian are expressed using the shorthand notations $\phi_j \triangleq \phi_j(\Phi_{j-1}(X, \theta))$ and $\phi'_j \triangleq \phi'_j(\Phi_{j-1}(X, \theta))$, respectively, and $\phi'_j : \mathbb{R}^{L_j} \rightarrow \mathbb{R}^{L_j \times L_j}$ is defined as $\phi'_j(y) \triangleq \frac{\partial}{\partial \varrho} \phi_j(\varrho)|_{\varrho=y}$, for all $y \in \mathbb{R}^{L_j}$. To facilitate the subsequent development and analysis, the following assumption is made on the activation functions.

Assumption 1. For each $j \in \{0, \dots, k\}$, the activation function ϕ_j , its Jacobian ϕ'_j , and Hessian $\phi''_j(y) \triangleq \frac{\partial^2}{\partial y^2} \phi_j(y)$ are bounded as

$$\begin{aligned} \|\phi_j(y)\| &\leq \mathfrak{a}_1 \|y\| + \mathfrak{a}_0, \\ \|\phi'_j(y)\| &\leq \mathfrak{b}_0, \\ \|\phi''_j(y)\| &\leq \mathfrak{c}_0, \end{aligned} \quad (3)$$

where $\mathfrak{a}_0, \mathfrak{a}_1, \mathfrak{b}_0, \mathfrak{c}_0 \in \mathbb{R}_{\geq 0}$ are known constants.

Remark 1. Most activation functions used in practice satisfy Assumption 1. Specifically, sigmoidal activation functions (e.g., logistic function, hyperbolic tangent etc.) have $\|\phi_j(y)\|$, $\|\phi'_j(y)\|$, and $\|\phi''_j(y)\|$ bounded uniformly by constants. Smooth approximations of rectified linear unit (ReLUs) such as Swish grow linearly, and hence satisfy the bound $\|\phi_j(y)\| \leq \mathfrak{a}_1 \|y\| + \mathfrak{a}_0$ of Assumption 1.

II. CONTINUOUS-TIME NONLINEAR REGRESSION

Various applications spanning across the domains of system identification, fault detection, financial time-series prediction, neuroscience, environmental predictions, medical diagnostics etc. require online identification of the underlying processes. Many such processes can be represented as a continuous-time nonlinear regression. Therefore, consider the NRE,

$$y(t) = f(x(t)) + \delta(t) \quad (4)$$

for all $t \in \mathbb{R}_{\geq 0}$, where $x(t) \in \Omega$ denotes a known input to the regression and lies in the compact set $\Omega \subset \mathbb{R}^m$, $y(t) \in \mathbb{R}^n$ denotes the output of the regression with available measurements, $f : \Omega \rightarrow \mathbb{R}^n$ denotes an unknown continuously differentiable function, and $\delta(t) \in \mathbb{R}^n$ denotes a bounded disturbance with known bound $\bar{\delta} \in \mathbb{R}_{>0}$ such that $\|\delta(t)\| \leq \bar{\delta}$ for all $t \in \mathbb{R}_{\geq 0}$. For notational brevity, time-dependencies on all signals will be suppressed in the subsequent development. Because the function f is unknown and has no known structure, there are challenges in learning the NRE. DNNs are a powerful tool for approximating such

unknown functions over compact sets, due to their universal function approximation property [31]. Therefore, consider a DNN $\Phi : \mathbb{R}^m \times \mathbb{R}^\rho \rightarrow \mathbb{R}^n$. Then a DNN-based approximation of (4) is given by

$$\hat{f} = \Phi(x, \hat{\theta}), \quad (5)$$

where $\hat{\theta} \in \mathbb{R}^\rho$ denotes the DNN parameter estimates that are designed based on the subsequent Lyapunov-based stability analysis. The objective is to find the best estimates of $\hat{\theta}$ such that $x \mapsto \Phi(x, \hat{\theta})$ approximates $x \mapsto f(x)$ for any $x \in \Omega$. To quantify the DNN-based nonlinear regression objective, let the loss function $\mathcal{L} : \mathbb{R}^\rho \rightarrow \mathbb{R}_{\geq 0}$ be defined as

$$\mathcal{L}(\theta) \triangleq \int_{\Omega} \left(\|f(x) - \Phi(x, \theta)\|^2 + \sigma \|\theta\|^2 \right) d\mu(x), \quad (6)$$

where μ denotes the Lebesgue measure, $\sigma \in \mathbb{R}_{>0}$ denotes a regularizing constant, and the term $\sigma \|\theta\|^2$ represents L_2 regularization (also popularly known as ridge regression in the machine learning community) [32, Sec. 7.1.1]. Note that this loss function is defined independently of the time-dependent signal $t \mapsto x(t)$ because the objective is to ensure the approximation holds for any $x \in \Omega$ and not just the set of points traversed by $t \mapsto x(t)$. Additionally, a user-selected compact convex parameter search space Θ satisfying $0_\rho \in \Theta$ and having a smooth boundary is considered. Additionally, $\bar{\theta} \triangleq \max_{\theta \in \Theta} \|\theta\| \in \mathbb{R}_{>0}$ is a bound on the user-defined search space. The objective is to identify the vector of ideal DNN parameters $\theta^* \in \Theta$ defined as

$$\theta^* \triangleq \arg \min_{\theta \in \Theta} \mathcal{L}(\theta). \quad (7)$$

Although using a bounded search space can restrict the optimality of the identified parameters to be local instead of global, it allows the subsequent development to be analyzed from a convex optimization perspective, which otherwise would be non-convex due to the nested NIP structure of DNNs. Specifically, due to the strict convexity of the regularizing term $\sigma \|\theta\|^2$ in (6), there exists $\sigma \in \mathbb{R}_{>0}$ which ensures $\mathcal{L}(\theta)$ is convex for all $\theta \in \Theta$. Additionally, the regularizing term has other advantages such as mitigation of overfitting [32, Sec. 7.1.1]. However, selecting very high values of σ can obscure the contribution of the $\|f(x) - \Phi(x, \theta)\|^2$ term to the loss function while also causing underfitting [32, Sec. 7.1.1]; therefore, there is a tradeoff between selecting low vs. high values of σ . Furthermore, note that that local minima for the $\|f(x) - \Phi(x, \theta)\|^2$ term are ubiquitous for various applications of DNNs. The important question is whether there are local minima of higher cost than the global minima. As noted in [32, Sec. 8.2.2.], this question remains open for general DNN architectures. However, for some DNN architectures, it has been established that every local minima is a global minima. For example, [33] established this property for deep residual neural networks (ResNets) with arbitrary nonlinear activation functions. Results such as [34] and [35] have concluded the same for DNNs with linear

activation functions, and [36] establishes the same for single-hidden-layer deep convolutional neural networks with rectified linear unit (ReLU) activation functions. Furthermore, from a practical standpoint, it is acceptable to find a point in the parameter space that has low but not necessarily minimal cost [32, Sec. 8.2.2.]. Therefore, we restrict our attention to the problem of finding a local minima. However, even this problem is challenging because a DNN parameterization can be represented using multiple equivalent parameterizations.

Example 1. Consider a scalar input-output NN with one hidden linear and one hidden neuron, $\Phi(x, \theta) = w_1 w_0 x$, where w_1 and w_0 are scalar NN weights. Then, for any $\alpha \in \mathbb{R}_{>0}$, defining the new weights $v_1 = \alpha w_1$ and $v_0 = \frac{w_0}{\alpha}$ yields an equivalent parameterization $\Phi(x, \theta) = v_1 v_0 x$ with different weights.

This equivalence leads to model identifiability issues, where the presence of uncountably infinite indistinguishable local minima can make the problem of identifying θ^* ill-posed [32, Sec. 8.2.2.]. To address this issue, the following subsection provides identifiability conditions for DNNs.

A. Identifiability Conditions

To define the conditions under which the problem of identifying θ^* is well-posed, we provide a definition of least squares identifiability, which is a modified version of [37, Definition 3] tailored to the regression problem in (4).

Definition 1. The parameter vector θ^* is identifiable over the set Θ if and only if it is a unique minimizer of \mathcal{L} over Θ . If θ^* is only an isolated local minimizer (i.e., if there exists an arbitrarily small neighborhood of θ^* where it is a unique minimizer), then θ^* is termed locally identifiable. If θ^* is identifiable over the entire Euclidean space \mathbb{R}^ρ , then it is globally identifiable.

For general deep learning tasks, achieving global identifiability can be intractable due to the aforementioned reasons for why we consider a bounded search space; therefore, we examine conditions such that θ^* is locally identifiable or identifiable over Θ . To obtain the conditions under which θ^* is identifiable over Θ , strict convexity is imposed on \mathcal{L} . Because Θ is a convex set, imposing strict convexity on \mathcal{L} ensures unique solutions to (7). A sufficient condition for ensuring strict convexity is ensuring the Hessian $\frac{\partial^2 \mathcal{L}}{\partial \theta^2}$ is positive definite, i.e., $\frac{\partial^2 \mathcal{L}}{\partial \theta^2} \succ 0$ for all $\theta \in \Theta$ [38, Sec. 3.1.4]. Imposing positive-definiteness on $\frac{\partial^2 \Phi}{\partial \theta^2}$ yields the condition

$$\int_{\Omega} (\Phi'^\top(x, \theta) \Phi'(x, \theta) + \sigma I_\rho) d\mu(x) - \int_{\Omega} \frac{\partial^2 \Phi(x, \theta)}{\partial \theta^2} (f(x) - \Phi(x, \theta)) d\mu(x) \succ 0, \quad (8)$$

for all $\theta \in \Theta$. Although the inequality in (8) offers an identifiability condition, this condition is challenging to verify because it involves a partial integro-differential inequality consisting of the unknown function approximation error $f(x) - \Phi(x, \theta)$ and the second-derivative of the DNN

$\frac{\partial^2 \Phi(x, \theta)}{\partial \theta^2}$ which is often computationally intractable. However, stricter conditions can be imposed to obtain tractable sufficient conditions for identifiability. To derive these stricter conditions, notice the term $\frac{\partial^2 \Phi(x, \theta)}{\partial \theta^2} (f(x) - \Phi(x, \theta))$ is bounded for all $x \in \Omega$ and $\theta \in \Theta$; this fact can be established by noticing the terms $\frac{\partial^2 \Phi(x, \theta)}{\partial \theta^2}$ and $f(x) - \Phi(x, \theta)$ are bounded for all $x \in \Omega$ and $\theta \in \Theta$ due to Φ being \mathcal{C}^2 and f being continuous. Therefore, let $\bar{\sigma} \in \mathbb{R}_{>0}$ denote the bound $\bar{\sigma} \triangleq \sup_{x \in \Omega, \theta \in \Theta} \left\| \frac{\partial^2 \Phi(x, \theta)}{\partial \theta^2} (f(x) - \Phi(x, \theta)) \right\|$. Then, a stricter condition for identifiability is obtained as

$$\int_{\Omega} (\Phi'^\top(x, \theta) \Phi'(x, \theta) + \sigma I_\rho - \bar{\sigma} I_\rho) d\mu(x) \succ 0. \quad (9)$$

Remark 2. Selecting a large regularizing constant σ can trivially ensure the condition in (9). However, doing so is undesirable as it obscures the DNN's contribution to the loss function in (6). Instead, it is desirable that the term $\int_{\Omega} \Phi'^\top(x, \theta) \Phi'(x, \theta) d\mu(x)$ contributes to achieving the identifiability condition in (9), which yields the condition $\int_{\Omega} \Phi'^\top(x, \theta) \Phi'(x, \theta) d\mu(x) \succ \bar{\sigma} I_\rho \mu(\Omega)$. Note that this condition, although still computationally intensive, is relatively easier to verify using a discrete approximation of the integral as compared to (9). Alternatively, a more conservative approach can be taken where σ is selected to be equal to $\bar{\sigma}$ while requiring only positive-definiteness to be verified for $\int_{\Omega} \Phi'^\top(x, \theta) \Phi'(x, \theta) d\mu(x)$.

The following lemma provides equivalent conditions for verifying if $\int_{\Omega} \Phi'^\top(x, \theta) \Phi'(x, \theta) d\mu(x)$ is positive definite to check for identifiability.

Lemma 1. Let $\sigma = \bar{\sigma}$. Then θ^* is identifiable over Θ if any of the following equivalent conditions are satisfied,

- i) $\int_{\Omega} \Phi'^\top(x, \theta) \Phi'(x, \theta) d\mu(x) \succ 0$ for all $\theta \in \Theta$,
- ii) there exists $x_1, \dots, x_\rho \in \Omega$ such that $\sum_{i=1}^{\rho} \Phi'^\top(x_i, \theta) \Phi'(x_i, \theta) \succ 0$ for all $\theta \in \Theta$,
- iii) there exists $x_1, \dots, x_\rho \in \Omega$ such that $\text{rank}([\Phi'^\top(x_1, \theta), \dots, \Phi'^\top(x_\rho, \theta)]) = \rho$ for all $\theta \in \Theta$.

Proof: Condition i) follows from (9) as stated before. By the definition of positive-definiteness of a matrix, condition i) is equivalent to stating $\int_{\Omega} v^\top \Phi'^\top(x, \theta) \Phi'(x, \theta) v d\mu(x) = \int_{\Omega} \|\Phi'(x, \theta) v\|^2 d\mu(x) > 0$ for all $v \neq 0_\rho$. Furthermore, consider an arbitrary partition of Ω formed by sets $\Omega_1, \dots, \Omega_\rho \subset \Omega$. Then the integral $\int_{\Omega} \|\Phi'(x, \theta) v\|^2 d\mu(x)$ can be upper-bounded as $\int_{\Omega} \|\Phi'(x, \theta) v\|^2 d\mu(x) \leq \sum_{i=1}^{\rho} \left(\sup_{x \in \Omega_i} \|\Phi'(x, \theta) v\|^2 \right) \mu(\Omega_i)$. Since $\sup_{x \in \Omega_i} \|\Phi'(x, \theta) v\|^2$ and $\mu(\Omega_i)$ are non-negative, the Cauchy-Schwarz inequality can be applied which yields $\sum_{i=1}^{\rho} \left(\sup_{x \in \Omega_i} \|\Phi'(x, \theta) v\|^2 \right) \mu(\Omega_i) \leq \left(\sum_{i=1}^{\rho} \sup_{x \in \Omega_i} \|\Phi'(x, \theta) v\|^2 \right) \left(\sum_{i=1}^{\rho} \mu(\Omega_i) \right)$. Hence, condition i) implies $\left(\sum_{i=1}^{\rho} \sup_{x \in \Omega_i} \|\Phi'(x, \theta) v\|^2 \right) \left(\sum_{i=1}^{\rho} \mu(\Omega_i) \right) > 0$ for all $v \neq 0_\rho$. Due to the property of partitions $\sum_{i=1}^{\rho} \mu(\Omega_i) = \mu(\Omega) > 0$,

the inequality $\sum_{i=1}^{\rho} \sup_{x \in \Omega_i} \|\Phi'(x, \theta) v\|^2 > 0$ is obtained. Therefore, selecting $x_i = \arg \sup_{x \in \Omega_i} \|\Phi'(x, \theta) v\|^2$ yields $\sum_{i=1}^{\rho} \sup_{x \in \Omega_i} \|\Phi'(x, \theta) v\|^2 = \sum_{i=1}^{\rho} v^T \Phi'^T(x_i, \theta) \Phi'(x_i, \theta) v > 0$ for all $v \neq 0_{\rho}$, thus implying $\sum_{i=1}^{\rho} \Phi'^T(x_i, \theta) \Phi'(x_i, \theta) v > 0$ for all $\theta \in \Theta$. Hence, condition i) implies condition ii).

To establish that conditions i) and ii) are equivalent, we now establish that condition i) is also necessary to satisfy condition ii). We establish this by the method of contradiction. Thus, assume for the sake of contraction that condition i) is violated and condition ii) is satisfied. Due to the violation of condition i), $\int_{\Omega} \Phi'^T(x, \theta) \Phi'(x, \theta) d\mu(x)$ is not positive-definite but only positive semi-definite. In this case, there exists $v \neq 0_{\rho}$ such that $\int_{\Omega} \|\Phi'(x, \theta) v\|^2 d\mu(x) = 0$. Furthermore, notice that $\int_{\Omega} \|\Phi'(x, \theta) v\|^2 d\mu(x)$ can be lower-bounded as $0 \leq \sum_{i=1}^{\rho} \left(\inf_{x \in \Omega_i} \|\Phi'(x, \theta) v\|^2 \right) \mu(\Omega_i) \leq \int_{\Omega} \|\Phi'(x, \theta) v\|^2 d\mu(x)$. Therefore, if $\int_{\Omega} \|\Phi'(x, \theta) v\|^2 d\mu(x) = 0$, then $\sum_{i=1}^{\rho} \left(\inf_{x \in \Omega_i} \|\Phi'(x, \theta) v\|^2 \right) \mu(\Omega_i) = 0$, which is only possible when $\inf_{x \in \Omega_i} \|\Phi'(x, \theta) v\|^2 = 0$ for all $i \in \{1, \dots, \rho\}$. Since the partitions are arbitrary, this condition must apply for all possible partitions of Ω , i.e., there does not exist a method to partition Ω_i such that $\inf_{x \in \Omega_i} \|\Phi'(x, \theta) v\|^2 > 0$ for any $i \in \{1, \dots, \rho\}$. Since condition ii) is assumed to be satisfied, there exists $x_1, \dots, x_{\rho} \in \Omega$ such that $\sum_{i=1}^{\rho} \|\Phi'(x_i, \theta) v\|^2 > 0$, implying $\|\Phi'(x_i, \theta) v\|^2 > 0$ for at least one $i \in \{1, \dots, \rho\}$. For such an i , due to the continuity of $\|\Phi'(x_i, \theta) v\|^2$, there exists a neighborhood of x_i of radius $\epsilon \in \mathbb{R}_{>0}$ given by $\mathcal{N}_i \triangleq \{x \in \Omega : \|x - x_i\| \leq \epsilon\}$ such that $\|\Phi'(x, \theta) v\|^2 > 0$ for all $x \in \mathcal{N}_i$. Additionally, note that $\mu(\mathcal{N}_i) > 0$. Then partitioning Ω such that $\Omega_i = \mathcal{N}_i$ yields $\inf_{x \in \Omega_i} \|\Phi'(x, \theta) v\|^2 > 0$, thus leading to a contradiction with the implications of condition i). Therefore, one cannot violate condition i) and satisfy condition ii) simultaneously. Hence, condition i) is necessary and sufficient for condition ii).

Now we establish the equivalence between conditions ii) and iii). Notice that condition ii) holds if and only if $\text{rank}(\sum_{i=1}^{\rho} \Phi'^T(x_i, \theta) \Phi'(x_i, \theta)) = \rho$, which is equivalent to the statement $\ker(\sum_{i=1}^{\rho} \Phi'^T(x_i, \theta) \Phi'(x_i, \theta)) = \{0_{\rho}\}$ due to the rank-nullity theorem [39, Thm. 2.3]. Additionally, due to the property that $\ker(A + B) \supseteq \ker(A) \cap \ker(B)$ for any given matrices A and B , the condition $\ker(\sum_{i=1}^{\rho} \Phi'^T(x_i, \theta) \Phi'(x_i, \theta)) = \{0_{\rho}\}$ holds if and only if $\bigcap_{i=1}^{\rho} \ker(\Phi'^T(x_i, \theta) \Phi'(x_i, \theta)) = \{0_{\rho}\}$. Furthermore, note that $\ker(\Phi'^T(x_i, \theta) \Phi'(x_i, \theta)) = \ker(\Phi'(x_i, \theta))$ which is established as follows. For any vector $v \in \mathbb{R}^{\rho}$, if $\Phi'(x_i, \theta) v = 0_n$, then multiplying by $\Phi'^T(x_i, \theta)$ on both sides yields $\Phi'^T(x_i, \theta) \Phi'(x_i, \theta) v = 0_{\rho}$. Additionally, if $\Phi'^T(x_i, \theta) \Phi'(x_i, \theta) v = 0_{\rho}$, then multiplying by v^T on both sides yields $v^T \Phi'^T(x_i, \theta) \Phi'(x_i, \theta) v = 0$,

equivalent to $\|\Phi'(x_i, \theta) v\| = 0$ which holds if and only if $\Phi'(x_i, \theta) v = 0_n$. Therefore, $\Phi'^T(x_i, \theta) \Phi'(x_i, \theta) v = 0_{\rho}$ if and only if $\Phi'(x_i, \theta) v = 0_{\rho}$, thus implying $\ker(\Phi'^T(x_i, \theta) \Phi'(x_i, \theta)) = \ker(\Phi'(x_i, \theta))$. Therefore, condition ii) is equivalent to the condition $\bigcap_{i=1}^{\rho} \ker(\Phi'(x_i, \theta)) = \{0_{\rho}\}$, which holds if and only if there exists no vector $v \neq 0_{\rho}$ such that $\Phi'(x_i, \theta) v = 0_n$ for all $i \in \{1, \dots, \rho\}$. This condition can hold if and only if the matrix $[\Phi'^T(x_1, \theta), \dots, \Phi'^T(x_{\rho}, \theta)]^T$ has ρ linearly independent columns, which is equivalent to the statement in condition iii) that $\text{rank}([\Phi'^T(x_1, \theta), \dots, \Phi'^T(x_{\rho}, \theta)]) = \rho$. Therefore, conditions ii) and iii) are equivalent, thus establishing the equivalence between conditions i)-iii). ■

Remark 3. To determine local identifiability (i.e., identifiability in an arbitrarily small neighborhood of θ^* as defined in Definition 1) instead of identifiability over Θ , the conditions i)-iii) stated in Lemma 1 can be relaxed to hold only at θ^* instead of holding for all $\theta \in \Theta$. Furthermore, $\bar{\sigma}$ can be redefined as $\bar{\sigma} = \sup_{x \in \Omega} \left\| \frac{\partial^2 \Phi(x, \theta^*)}{\partial \theta^2} (f(x) - \Phi(x, \theta^*)) \right\|$ to check for local identifiability. This redefinition of $\bar{\sigma}$ is expected to yield a significantly smaller value than its previous definition because it does not involve the supremum to be computed over the entire Θ but only at θ^* .

Remark 4. Notice that the universal function approximation theorem for DNNs was not invoked in the definition of θ^* or in the derivation of the identifiability conditions. The universal function approximation theorem [31, Theorem 3.1] states that the function space of DNNs is dense in the space of continuous functions $\mathcal{C}(\Omega)$. As a result, for any prescribed $\varepsilon > 0$, there exists a DNN Φ and a corresponding parameter θ such that $\sup_{x \in \Omega} \|f(x) - \Phi(x, \theta)\| < \varepsilon$, and therefore $\int_{\Omega} \|f(x) - \Phi(x, \theta)\|^2 d\mu(x) < \varepsilon^2 \mu(\Omega)$. However, it is not known how to obtain a bound $\bar{\theta}$ on such parameter θ for an arbitrary ε , which causes difficulties in constructing the bounded search space Θ . Therefore, we allow the user-defined search space Θ to be arbitrarily selected in the above analysis, at the loss of guarantees on the approximation accuracy. Although the constant ε that bounds $\sup_{x \in \Omega} \|f(x) - \Phi(x, \theta^*)\|$ might no longer be arbitrary in this case, it would still be finite due to the continuity of f and Φ , where minimizing (6) would yield the best regularized approximation of f . Therefore, the unknown nonlinear function can be modeled as

$$f(x) = \Phi(x, \theta^*) + \varepsilon(x), \quad (10)$$

where $\varepsilon(x) \triangleq f(x) - \Phi(x, \theta^*)$ is bounded by $\bar{\varepsilon}$ as $\|\varepsilon(x)\| \leq \bar{\varepsilon}$ for all $x \in \Omega$.

Recent work [27] provided identifiability conditions for linear regression equations (LREs) where there is a LIP model and showed that it is equivalent to finite-time excitation (FE) or interval excitation (IE) conditions. The IE/FE condition is known to be strictly weaker than the persistence of excitation (PE) condition. Therefore, adaptive methods such as CL (and other methods discussed in the Introduction) that achieve parameter identification under only

the IE/FE conditions can be interpreted to leverage only the identifiability of the parameters. In this context, the conditions in Lemma 1 can be viewed as a generalization of the identifiability conditions in [27] to NREs where there is an NIP model. This observation raises the question whether an adaptive estimation technique can be developed to identify θ^* under the sufficient identifiability conditions stated in Lemma 1, as opposed to the more stringent PE condition. Our paper answers this question with an affirmative by developing a CL-based adaptive estimator for θ^* .

Before providing the CL-based estimator development, we provide a brief overview of the gradient-based estimators for DNNs for better context. For the loss function in (6), the corresponding loss density is given by $\mathcal{L}(\hat{\theta}) = \|f(x) - \Phi(x, \hat{\theta})\|^2 + \sigma \|\hat{\theta}\|^2$. Then the gradient-based estimator is derived by formulating the negative gradient flow of $\mathcal{L}(\hat{\theta})$ given by

$$\begin{aligned}\dot{\hat{\theta}} &= -\Gamma \nabla_{\hat{\theta}} \mathcal{L}(\hat{\theta}) \\ &= -\Gamma \sigma \hat{\theta} - \Gamma \Phi'^\top(x, \hat{\theta}) \tilde{y},\end{aligned}\quad (11)$$

where $\Gamma \in \mathbb{R}^{\rho \times \rho}$ denotes the adaptation gain, and

$$\tilde{y} \triangleq y(t) - \Phi(x, \hat{\theta}) \quad (12)$$

denotes the regression error. Using a similar approach as in [4] and [5], $\hat{\theta}$ converges to a neighborhood of θ^* provided the PE condition is satisfied. The PE condition requires that there exist some $T \in \mathbb{R}_{>0}$ such that $\int_{\underline{t}}^{\underline{t}+T} \Phi'^\top(x(\tau), \hat{\theta}(\tau)) \Phi'(x(\tau), \hat{\theta}(\tau)) d\tau \succ 0$ for all $\underline{t} \in \mathbb{R}_{\geq 0}$, which is restrictive because the positive definiteness has to hold on a moving time window for all time. In contrast, Lemma 1 suggests that θ^* is identifiable if $t \rightarrow x(t)$ traverses through points $x_1, \dots, x_\rho \in \Omega$ such that conditions ii) or iii) of Lemma 1 is satisfied. Specifically, if $t \rightarrow x(t)$ is shaped to traverse through such points $x_1, \dots, x_\rho \in \Omega$ in a finite-time interval, it must be possible to develop an adaptive estimator to identify θ^* without requiring PE. Based on this insight, we provide CL-based adaptive update laws in the following section.

B. Concurrent Learning Algorithm for Continuous-Time Regression Problems

Consider the NRE in (4). Using (1), Remark 4, and (10), the regression error in (12) can be represented as

$$\tilde{y}(x) = \Phi(x, \theta^*) + \varepsilon(x) + \delta(t) - \Phi(x, \hat{\theta}). \quad (13)$$

Therefore, the parameter identification objective is to minimize the parameter estimation error, defined as

$$\tilde{\theta} \triangleq \theta^* - \hat{\theta}, \quad (14)$$

where θ^* is defined in (7) and $\hat{\theta}$ represents the parameter estimates. Using the definitions of $\Phi(x, \theta^*)$ and $\Phi(x, \hat{\theta})$, a first-order Taylor series approximation-based model of the estimation error is used to obtain [3]

$$\Phi(x, \theta^*) - \Phi(x, \hat{\theta}) = \Phi'(x, \hat{\theta})\tilde{\theta} + R(x, \tilde{\theta}), \quad (15)$$

where $R(x, \tilde{\theta})$ represents the Lagrange remainder term.

1) *Concurrent Learning (CL) Adaptation Laws for Non-linear Regression:* Two Lyapunov-based adaptation laws which harness different properties of DNNs are developed to achieve the parameter identification objective. The first adaptation law is formulated by drawing on established methodologies in CL using the known input and estimated representation of the system dynamics, where the estimated representation is formulated using the output of the DNN. The discrepancy between the known input and the reconstructed version are then stored in a history stack which provides a richer data-set that incorporates previous information into the update law. The second adaptation law uses similar motivation for the history stack construction; however, it directly incorporates the Jacobian of the DNN into the update process, leveraging the DNN's internal dynamics, instead of the output, in the history stack construction.

a) *Weight Adaptation Law Algorithm 1:* The first adaptation law is developed using traditional CL techniques which allows the adaptation to be guided by the output of the DNN. The Jacobian of the DNN is denoted $\Phi'(x, \hat{\theta})$ and the Jacobian of the DNN at a specified point x_i and the current state estimates is denoted $\Phi'(x_i, \hat{\theta})$. The core idea is to leverage the recorded input-output data to refine the parameter estimates. The implementable form of the CL-DNN update law is designed as

$$\dot{\hat{\theta}} = \text{proj} \left(\gamma_1 \sum_{i=1}^N \Phi'^\top(x_i, \hat{\theta}) (y_i - \hat{y}_i) - \gamma_2 \hat{\theta} \right), \quad (16)$$

where $\gamma_1, \gamma_2 \in \mathbb{R}^{\rho \times \rho}$ denote positive-definite user-selected adaptation gain matrices and the projection operator is a smooth projection operator defined in [40, Appendix E] which ensures that the adaptive estimate remains within the bounded parameter search space Θ . An analytical form of the implementable weight update law can be obtained using (12), (13), and (15) as

$$\begin{aligned}\dot{\hat{\theta}} &= \text{proj} \left(\gamma_1 \sum_{i=1}^N \Phi'^\top(x_i, \hat{\theta}) (\Phi'(x_i, \hat{\theta})\tilde{\theta}) - \gamma_2 \hat{\theta} \right. \\ &\quad \left. + \gamma_1 \sum_{i=1}^N \Phi'^\top(x_i, \hat{\theta}) (R(x_i, \tilde{\theta}) + \varepsilon(x_i) + \delta(t)) \right).\end{aligned}\quad (17)$$

b) *Weight Adaptation Law Algorithm 2:* The second weight adaptation law is developed based on the desire to leverage the internal dynamics of the DNN. The implementable form of the second CL-DNN update law is designed as

$$\dot{\hat{\theta}} = \text{proj} \left(\gamma_1 \sum_{i=1}^N \Phi'^\top(x_i, \hat{\theta}) (y_i + \Phi'(x_i, \hat{\theta})\tilde{\theta}) - \gamma_2 \hat{\theta} \right). \quad (18)$$

The analytical form of the weight adaptation law can be obtained by substituting (4), (10), and (15) into (18) which

yields

$$\begin{aligned}\dot{\hat{\theta}} = & \text{proj} \left(-\gamma_2 \hat{\theta} + \gamma_1 \sum_{i=1}^N \Phi'^\top(x_i, \hat{\theta}) \left(\Phi(x_i, \hat{\theta}) + \Phi'(x_i, \hat{\theta}) \hat{\theta} \right. \right. \\ & \left. \left. + R(x_i, \tilde{\theta}_i) + \varepsilon(x_i) + \delta(t) - \Phi'(x_i, \hat{\theta}) \hat{\theta} \right) \right). \quad (19)\end{aligned}$$

Using a first-order Taylor series approximation-based model between the DNN estimate and the DNN with a 0_ρ weight vector yields

$$-\Phi(x_i, \hat{\theta}) = -\Phi(x_i, 0_\rho) - \Phi'(x_i, \hat{\theta}) \hat{\theta} + R(x_i, \hat{\theta}_i). \quad (20)$$

Based on the definition in (2), the output of the DNN with all the weights and biases prescribed as 0_ρ is $\Phi(x_i, 0_\rho) = 0_n$. Using (20), (49), and canceling cross terms yields

$$\begin{aligned}\dot{\hat{\theta}} = & \text{proj} \left(\gamma_1 \sum_{i=1}^N \Phi'^\top(x_i, \hat{\theta}) \left(R(x_i, \tilde{\theta}_i) - R(x_i, \hat{\theta}_i) + \varepsilon(x_i) \right) \right. \\ & \left. + \delta(t) + \gamma_1 \sum_{i=1}^N \Phi'^\top(x_i, \hat{\theta}) \Phi'(x_i, \hat{\theta}) \tilde{\theta} - \gamma_2 \hat{\theta} \right). \quad (21)\end{aligned}$$

The update laws developed in (16) and (18) are evaluated with their respective analytical forms in (17) and (21) in a Lyapunov-based stability analysis in the following section.

C. Stability Analysis

Using [41], the Lagrange remainder in (15) is bounded as

$$\|R(x, \tilde{\theta})\| \leq \rho_0(\|x\|) \|\tilde{\theta}\|^2, \quad (22)$$

where $\rho_0(\|x\|) : \mathbb{R}_{\geq 0} \rightarrow \mathbb{R}_{\geq 0}$ is a strictly increasing quadratic polynomial of the form $\rho_0(\|x\|) = a_2 \|x\|^2 + a_1 \|x\| + a_0$ with some constants $a_2, a_1, a_0 \in \mathbb{R}_{>0}$. Similarly, the Lagrange remainder for (20) can be expressed as $\|R(x, \hat{\theta})\| \leq \rho_0(\|x\|) \|\hat{\theta}\|^2$ which can be further bounded as

$$\|R(x, \hat{\theta})\| \leq \bar{\theta}^2 \rho_0(\|x\|). \quad (23)$$

Using [41], the Jacobian of the DNN can be bounded as

$$\|\Phi'(x, \hat{\theta})\| \leq \rho_1(\|x\|), \quad (24)$$

where $\rho_1 : \mathbb{R}_{\geq 0} \rightarrow \mathbb{R}_{\geq 0}$ denotes a strictly-increasing function. Due to the fact that $R(x, \tilde{\theta})$, $R(x, \hat{\theta})$, $\varepsilon(x)$, and $\delta(t)$, are bounded, the bounds $\|\Phi'^\top(x_i, \hat{\theta}) R(x_i, \tilde{\theta})\| \leq \rho_a(\|x_i\|) \|\tilde{\theta}\|^2$, $\|\Phi'^\top(x_i, \hat{\theta}) (\varepsilon(x_i) + \delta(t))\| \leq \rho_b(\|x_i\|)$, and $\|\Phi'^\top(x_i, \hat{\theta}) (\varepsilon(x_i) + \delta(t) - R(x_i, \hat{\theta}))\| \leq \rho_c(\|x_i\|)$ hold where $\rho_a, \rho_b, \rho_c : \mathbb{R}_{\geq 0} \rightarrow \mathbb{R}_{\geq 0}$ denote strictly-increasing bounding functions.

Let $\lambda_1 \triangleq \frac{\gamma_2}{2} - \gamma_1 + \gamma_1 \left(\lambda_{\min} \left\{ \sum_{i=1}^N \Phi'^\top(x_i, \hat{\theta}) \Phi'(x_i, \hat{\theta}) \right\} \right)$, $\lambda_{1d} \in \mathbb{R}_{\geq 0}$ be the desired convergence rate, and constants $\iota_2, \iota_2 \in \mathbb{R}_{>0}$ be defined as $\iota_1 \triangleq \frac{\gamma_2}{2} \bar{\theta}^2 + \frac{\gamma_1}{2} \left(\sum_{i=1}^N \rho_b(\|x_i\|) \right)^2$, $\iota_2 = \frac{\gamma_2}{2} \bar{\theta}^2 + \frac{\gamma_1}{2} \left(\sum_{i=1}^N \rho_c(\|x_i\|) \right)^2$.

Assumption 2. There exists $\lambda_e > 0$ and there exists $T > 0$ for all $t \geq T$ such that $\lambda_{\min} \left\{ \sum_{i=1}^N \Phi'^\top(X_i, \hat{\theta}) \Phi'(X_i, \hat{\theta}) \right\} \geq \lambda_e$.

Remark 5. Since $\lambda_{\min} \left\{ \sum_{i=1}^N \Phi'^\top(X_i, \hat{\theta}) \Phi'(X_i, \hat{\theta}) \right\}$ is positive under Assumption 2 and is lower-bounded by λ_e , an increase in λ_e results in a larger value for λ_1 being obtained, which implies faster convergence. If Assumption 2 does not hold, the gain γ_2 , which is based on the sigma modification technique in [42, Sec. 8.4.1], helps achieve the boundedness of $\tilde{\theta}$ in the stability result. However, selecting a high gain for γ_2 can deteriorate tracking and parameter estimation performance because it yields a higher value for ι_1 and ι_2 , leading to larger ultimate bounds given by $\sqrt{\frac{\iota_1}{\lambda_{1d}}}$ and $\sqrt{\frac{\iota_2}{\lambda_{1d}}}$, respectively.

Remark 6. The subsequent theorems, establish ultimate boundedness for the error signals, rather than the stronger property of uniform ultimate boundedness (UUB). This distinction, where the characteristics of the ultimate bound depend on the initial conditions, is a known consequence of relaxing the PE condition, as observed in the related literature [25] and [43]. In this result, the dependence on the initial conditions is primarily due to the history stack which is populated by the system states which evolve as a function of the initial condition.

To facilitate the stability analysis, let the candidate Lyapunov function $V : \mathbb{R}^\rho \rightarrow \mathbb{R}_{\geq 0}$ be defined as

$$V(\tilde{\theta}) = \frac{1}{2} \tilde{\theta}^\top \tilde{\theta}. \quad (25)$$

Taking the time derivative of $V(\tilde{\theta})$ yields

$$\dot{V}(\tilde{\theta}) = \tilde{\theta}^\top \dot{\tilde{\theta}}. \quad (26)$$

Theorem 1 and Theorem 2 provide convergence guarantees for the parameter estimation errors for the update laws in (17) and (21), respectively.

Theorem 1. For the parameter identification objective defined in (14), the adaptation law developed in (17) ensures that the parameter estimation error $\tilde{\theta}$ is bounded in the sense that $\|\tilde{\theta}(t)\| \leq \sqrt{\|\tilde{\theta}(t_0)\|^2 e^{-2\lambda_{1d}(t-t_0)} + \frac{\iota_1}{\lambda_{1d}} (1 - e^{-2\lambda_{1d}t})}$, for all $t \in \mathbb{R}_{\geq 0}$, provided $\lambda_1 > \lambda_{1d} + \frac{\gamma_1}{2} \rho_a^2(\|x_i\|) \|\tilde{\theta}(t_0)\|^2$.

Proof: Consider the candidate Lyapunov function in (25). From (17) and (26),

$$\begin{aligned}\dot{V}(\tilde{\theta}) = & -\tilde{\theta}^\top \left(\gamma_1 \sum_{i=1}^N \Phi'^\top(x_i, \hat{\theta}) \Phi'(x_i, \hat{\theta}) \tilde{\theta} + \gamma_2 (\tilde{\theta} - \theta^*) \right) \\ & + \gamma_1 \sum_{i=1}^N \Phi'^\top(x_i, \hat{\theta}) (R(x_i, \tilde{\theta}) + \varepsilon(x_i) + \delta(t))\end{aligned} \quad (27)$$

Upper bounding (27) yields

$$\begin{aligned}\dot{V}(\tilde{\theta}) &\leq - \left(\lambda_1 - \frac{\gamma_1}{2} \sum_{i=1}^N \rho_a^2(\|x_i\|) \|\tilde{\theta}\|^2 \right) \|\tilde{\theta}\|^2 \\ &\quad + \frac{\gamma_1}{2} \left(\sum_{i=1}^N \rho_b(\|x_i\|) \right) + \frac{\gamma_2}{2} \tilde{\theta}^2.\end{aligned}\quad (28)$$

When $\lambda_1 > \lambda_{1d} + \frac{\gamma_1}{2} \rho_a^2(\|x_i\|) \|\tilde{\theta}(t_0)\|^2$,

$$\dot{V}(\tilde{\theta}) \leq -\lambda_{1d} \|\tilde{\theta}\|^2 + \iota_1. \quad (29)$$

The inequality in (29) can be further bounded as $V(\tilde{\theta}(t)) \leq V(\tilde{\theta}(t_0)) e^{-\lambda_{1d}(t-t_0)} + \frac{\iota_1}{\lambda_{1d}} (1 - e^{-\lambda_{1d}t})$. Then, [44, Def. 4.6] can be invoked to conclude that $\tilde{\theta}$ is bounded such that $\|\tilde{\theta}(t)\| \leq \sqrt{\|\tilde{\theta}(t_0)\|^2 e^{-2\lambda_{1d}(t-t_0)} + \frac{\iota_1}{\lambda_{1d}} (1 - e^{-2\lambda_{1d}t})}$. Using (25) and (29) implies $\tilde{\theta} \in \mathcal{L}_\infty$. Additionally, due to the use of the projection operator, $\hat{\theta} \in \mathcal{L}_\infty$. ■

Theorem 2. For the parameter identification objective defined in (14), the adaptation law developed in (17) ensures that the parameter estimation error $\tilde{\theta}$ is bounded in the sense that $\|\tilde{\theta}(t)\| \leq \sqrt{\|\tilde{\theta}(t_0)\|^2 e^{-2\lambda_{1d}(t-t_0)} + \frac{\iota_2}{\lambda_{1d}} (1 - e^{-2\lambda_{1d}t})}$, for all $t \in \mathbb{R}_{\geq 0}$ provided $\lambda_1 > \lambda_{1d} + \frac{\gamma_1}{2} \rho_a^2(\|x_i\|) \|\tilde{\theta}(t_0)\|^2$.

Proof: Consider the candidate Lyapunov function in (25). From (26) and (21),

$$\begin{aligned}\dot{V}(\tilde{\theta}) &= -\tilde{\theta}^\top \left(\gamma_2 \tilde{\theta} - \gamma_2 \theta^* \right. \\ &\quad \left. + \gamma_1 \sum_{i=1}^N \Phi'^\top(x_i, \hat{\theta}) \left(\Phi'(x_i, \hat{\theta}) \tilde{\theta} + \varepsilon(x_i) \right. \right. \\ &\quad \left. \left. - R(x_i, \tilde{\theta}) - R(x_i, \hat{\theta}) + \delta(t) \right) \right),\end{aligned}\quad (30)$$

and $\dot{V}(\tilde{\theta})$ can be upper bounded as

$$\dot{V}(\tilde{\theta}) \leq - \left(\lambda_1 - \frac{\gamma_1}{2} \sum_{i=1}^N \rho_a^2(\|x_i\|) \|\tilde{\theta}\|^2 \right) \|\tilde{\theta}\|^2 + \iota_2. \quad (31)$$

When $\lambda_1 > \lambda_{1d} + \frac{\gamma_1}{2} \sum_{i=1}^N \rho_a^2(\|x_i\|) \|\tilde{\theta}(t_0)\|^2$,

$$\dot{V}(\tilde{\theta}) \leq -\lambda_{1d} \|\tilde{\theta}\|^2 + \iota_2.$$

As a result, $V(\tilde{\theta})$ can be further bounded as $V(\tilde{\theta}(t)) \leq V(\tilde{\theta}(t_0)) e^{-\lambda_{1d}(t-t_0)} + \frac{\iota_2}{\lambda_{1d}} (1 - e^{-\lambda_{1d}t})$. Then, [44, Def. 4.6] can be invoked to conclude that $\tilde{\theta}$ is bounded such that $\|\tilde{\theta}(t)\| \leq \sqrt{\|\tilde{\theta}(t_0)\|^2 e^{-2\lambda_{1d}(t-t_0)} + \frac{\iota_2}{\lambda_{1d}} (1 - e^{-2\lambda_{1d}t})}$. Using (25) and (31) implies $\tilde{\theta} \in \mathcal{L}_\infty$, and by use of the projection operator, $\hat{\theta} \in \mathcal{L}_\infty$. ■

III. UNKNOWN SYSTEM DYNAMICS AND CONTROL DESIGN

Consider a control-affine nonlinear dynamic system modeled as

$$\dot{x} = f(x, \dot{x}) + u, \quad (32)$$

where $x, \dot{x} \in \mathbb{R}^n$ denotes the measurable generalized position and velocity, $f : \mathbb{R}^n \rightarrow \mathbb{R}^n$ denotes an unknown continuously differentiable function, and $u \in \mathbb{R}^n$ denotes a control input. The tracking control objective is to simultaneously track a user-defined reference trajectory $x_d \in \mathbb{R}^n$ and learn the unknown function $f(x, \dot{x})$ online using a DNN beginning at the initial time denoted t_0 . Therefore, an unknown function $f(x, \dot{x})$ can be modeled as

$$f(x, \dot{x}) = \Phi(X, \theta^*) + \varepsilon(X), \quad (33)$$

where the ideal DNN estimate is denoted $\Phi(X, \theta^*) \in \mathbb{R}^{L_{k+1}}$ where θ^* is defined in (7), and the input to the DNN is denoted $X \triangleq [x^\top, \dot{x}^\top]^\top$.

The reference trajectory is assumed to be sufficiently smooth (i.e., $\|x_d\| \leq \bar{x}_d$, $\|\dot{x}_d\| \leq \bar{\dot{x}}_d$, and $\|\ddot{x}_d\| \leq \bar{\ddot{x}}_d$), where $\bar{x}_d, \bar{\dot{x}}_d, \bar{\ddot{x}}_d \in \mathbb{R}_{>0}$ are known constant bounds. To quantify the tracking objective, the trajectory tracking errors $e, r \in \mathbb{R}^n$ are defined as

$$e \triangleq x - x_d, \quad (34)$$

$$r \triangleq \dot{e} + \alpha_1 e. \quad (35)$$

The structure of (35) is motivated by the subsequent stability analysis in Theorem 3 and Theorem 4 which indicate the boundedness of convergence of e can be determined from the boundedness and convergence of r . As a result, the following error system development, control design, and stability analysis are focused on the boundedness and convergence of r . Taking the time derivative of (35) and applying (32) yields the open-loop error system

$$\dot{r} = f(x, \dot{x}) + u - \ddot{x}_d + \alpha_1 \dot{e}. \quad (36)$$

The subsequent development considers the concurrent tracking control and system identification problem. It is desirable that the tracking objective defined in (34) is minimized. The parameter identification objective is to identify a set of parameters that minimizes the parameter estimation error defined in (14).

A. Closed-loop Error System and Control Law Development

Since $f(x, \dot{x})$ in (36) is unknown, we are motivated to develop an approximation that can be used as a feedforward control element. The uncertainty in $f(x, \dot{x})$ is not assumed to be modeled by uncertain linearly parameterizable terms; hence, approximation methods such as DNN are motivated. In this section, we design the controller and closed-loop error system to facilitate the subsequent development of online Lyapunov-based adaptive update laws for the Lb-CL-DNN and stability analysis. To this end, we substitute the DNN representation for f from (33) into (36) to yield

$$\dot{r} = \Phi(X, \theta^*) + \varepsilon(X) + u - \ddot{x}_d + \alpha_1 \dot{e}. \quad (37)$$

The control input is designed as

$$u = \ddot{x}_d - \Phi(X, \hat{\theta}) - k_1 r - e - \alpha_1 \dot{e}, \quad (38)$$

where $\hat{\theta} \in \mathbb{R}^p$ is an adaptive estimate of the parameter θ^* , and $k_1 \in \mathbb{R}_{>0}$ is a user-defined control gain. Using the definitions

of $\Phi(X, \theta^*)$ and $\Phi(X, \hat{\theta})$, substituting (38) and (15) onto (37) and canceling cross terms yields

$$\dot{r} = \Phi'(X, \hat{\theta})\tilde{\theta} + R(x, \tilde{\theta}) + \varepsilon(X) - k_1 r - e. \quad (39)$$

B. Dynamic State-Derivative Observer

Motivated by the desire to incorporate previous state information into the update law in a CL style, the update law is augmented with a history stack containing the error between the calculated control input and a reconstructed version of the control input. To reconstruct (32), an observer is developed to estimate the unmeasurable state \ddot{x} . The dynamic state-derivative observer is designed as

$$\dot{\hat{r}} = \hat{\Delta} - \ddot{x}_d + \alpha_1 \dot{e} + \alpha_2 \tilde{r}, \quad (40)$$

$$\dot{\hat{\Delta}} = \tilde{r} + k_{\Delta} \tilde{\Delta} - \dot{u}, \quad (41)$$

where $\hat{r}, \hat{\Delta} \in \mathbb{R}^n$ denote the observer estimates for r and \ddot{x} , respectively, $\tilde{r}, \tilde{\Delta} \in \mathbb{R}^n$ denote the observer errors, $\tilde{r} = r - \hat{r}$ and $\tilde{\Delta} = \ddot{x} - \hat{\Delta}$, respectively $\alpha, k_{\Delta} \in \mathbb{R}_{>0}$ denote constant observer gains, and \dot{u} is the unmeasurable derivative of the control input. Taking the time derivative of \tilde{r} and $\tilde{\Delta}$ and applying (40) and (41) yields

$$\dot{\tilde{r}} = \tilde{\Delta} - \alpha_2 \tilde{r}, \quad (42)$$

$$\dot{\tilde{\Delta}} = \dot{f}(x, \dot{x}) + \dot{u} - \tilde{r} - k_{\Delta} \tilde{\Delta} - \dot{u}, \quad (43)$$

where $\dot{f}(x, \dot{x}) \triangleq \frac{d}{dt} f(x, \dot{x}) = \frac{\partial f}{\partial x} \dot{x} + \frac{\partial f}{\partial \dot{x}} \ddot{x}$ and $\dot{u} \triangleq \frac{d}{dt} u$. The observer error \tilde{r} is known because r and \hat{r} are known. Because $\tilde{\Delta} = \dot{\tilde{r}} + \alpha_2 \tilde{r}$, the implementable form of (41) can be obtained by integrating on both sides and using the relation $\int_{t_0}^t \dot{\tilde{r}} = \tilde{r}(t) - \tilde{r}(t_0)$, which yields $\tilde{\Delta}(t) = \hat{\Delta}(t_0) + k_{\Delta}(\tilde{r}(t) - \tilde{r}(t_0)) - (u(t) - u(t_0)) + \int_{t_0}^t (k_{\Delta} \alpha_2 + 1) \tilde{r}(\tau) d\tau$.

Let the concatenated error vectors $z \in \mathbb{R}^{2n}$ and $\zeta \in \mathbb{R}^{\psi}$ be defined as $z \triangleq [\tilde{r}^{\top}, \tilde{\Delta}^{\top}]^{\top}$ and $\zeta \triangleq [r^{\top}, e^{\top}, \hat{\theta}^{\top}]^{\top}$, respectively, where $\psi \triangleq 2n + \rho$. Additionally, let the open and connected set $\mathcal{D} \subset \mathbb{R}^{\psi}$ be defined as $\mathcal{D} \triangleq \{\zeta \in \mathbb{R}^{\psi} : \|\zeta\| < \chi\}$, where $\chi \in \mathbb{R}_{>0}$ denotes a subsequently defined known upper bound. The following lemma establishes a bound on $\dot{f}(x, \dot{x})$ when $\zeta \in \mathcal{D}$ to facilitate the convergence analysis for the observer. The subsequent analysis in the main theorems will then provide additional conditions under which the trajectories $\zeta(t)$ stay within \mathcal{D} for all time $[t_0, \infty)$ using the combined controller-observer adaptation laws.

Lemma 2. For all $\zeta \in \mathcal{D}$, there exists a constant $\delta_f \in \mathbb{R}_{>0}$ such that the bound $\|\dot{f}(x, \dot{x})\| \leq \delta_f$ holds.

Proof: For all $\zeta \in \mathcal{D}$, $\|\zeta\| < \chi$, and hence $\|r\|, \|e\|, \|\hat{\theta}\| < \chi$. Since $\|x\| = \|e + x_d\| \leq \|e\| + \|x_d\| \leq \|e\| + \overline{x_d}$ and $\|\dot{x}\| = \|r - \alpha_1 e + \dot{x}_d\| \leq \|r\| + \alpha_1 \|e\| + \overline{x_d}$, the bounds $\|x\| \leq \chi + \overline{x_d}$ and $\|\dot{x}\| \leq (\alpha_1 + 1) \chi + \overline{x_d}$ hold for all $\zeta \in \mathcal{D}$. Similarly, $\|\hat{\theta}\| \leq \|\theta^*\| + \|\tilde{\theta}\| \leq \bar{\theta} + \chi$ for all $\zeta \in \mathcal{D}$. Moreover, using (32) and (38), $\ddot{x} = f(x, \dot{x}) - \Phi(X, \hat{\theta}) - k_1 r - e - \alpha_1 \dot{e} + \ddot{x}_d$. The terms $f(x, \dot{x})$ and $\Phi(X, \hat{\theta})$ can be bounded by a constant due to continuity of f and Φ and boundedness

of x , \dot{x} , and $\hat{\theta}$, for all $X \in \mathcal{D}$, because x , \dot{x} are bounded and using the definitions in (34) and (35), r , e and \dot{e} are bounded for all $X \in \mathcal{D}$ and \ddot{x}_d is bounded by design. Thus, there exists a constant $\overline{x} \in \mathbb{R}_{>0}$ such that $\|\ddot{x}\| \leq \overline{x}$ for all $\zeta \in \mathcal{D}$. Since $f(x, \dot{x})$ is continuously differentiable, there exist constants $\varrho_1, \varrho_2 \in \mathbb{R}_{>0}$ such that $\left\| \frac{\partial f}{\partial x} \right\| \leq \varrho_1$ and $\left\| \frac{\partial f}{\partial \dot{x}} \right\| \leq \varrho_2$ for all $\zeta \in \mathcal{D}$. Therefore, $\left\| \dot{f}(x, \dot{x}) \right\| \leq \left\| \frac{\partial f}{\partial x} \right\| \|\dot{x}\| + \left\| \frac{\partial f}{\partial \dot{x}} \right\| \|\ddot{x}\|$ and $\|\ddot{x}\| \leq \varrho_1 ((\alpha_1 + 1) \chi + \overline{x_d}) + \varrho_2 \overline{x}$. Therefore, selecting $\delta_f \triangleq \varrho_1 ((\alpha_1 + 1) \chi + \overline{x_d}) + \varrho_2 \overline{x}$ yields $\left\| \dot{f}(x, \dot{x}) \right\| \leq \delta_f$ for all $\zeta \in \mathcal{D}$. ■

Let $\Lambda_1 \triangleq \min \{k_{\Delta}, 2\alpha_2\}$. The following lemma establishes the convergence properties of the observer error system in (42) and (43).

Lemma 3. Consider the observer given by (40) and (41). The observer error is bounded in the sense that $\|z(t)\| \leq \sqrt{\|z(t_0)\|^2 e^{-\Lambda_1(t-t_0)} + \frac{\delta_f^2}{\Lambda_1} (1 - e^{-\Lambda_1 t})}$ for all $t \in \mathbb{R}_{\geq 0}$, provided $\zeta \in \mathcal{D}$. Moreover, the observer can achieve a prescribed accuracy $\delta_{\Delta} \in \mathbb{R}_{>0}$ with the settling time $t_{\Delta} \triangleq t_0 + \frac{1}{\Lambda_1} \ln \left(\frac{k_{\Delta} \Lambda_1 \|z(t_0)\|^2 - \delta_f^2}{k_{\Delta} \Lambda_1 \delta_{\Delta}^2 - \delta_f^2} \right)$, provided the feasibility gain condition $k_{\Delta} \Lambda_1 > \frac{\delta_f^2}{\delta_{\Delta}^2}$ is satisfied.

Proof: Consider the candidate Lyapunov function $\mathcal{V}_{\Delta}(z) \triangleq \frac{1}{2} \tilde{\Delta}^{\top} \tilde{\Delta} + \frac{1}{2} \tilde{r}^{\top} \tilde{r}$. Taking the derivative, using (42), (43), and canceling cross terms yields $\dot{\mathcal{V}}_{\Delta}(z) \leq -\tilde{\Delta}^{\top} k_{\Delta} \tilde{\Delta} - \tilde{r}^{\top} \alpha_2 \tilde{r} + \tilde{\Delta}^{\top} \dot{f}(x, \dot{x})$. Using Young's inequality and Lemma 2, $\dot{\mathcal{V}}_{\Delta}(z)$ can be further upper-bounded as $\dot{\mathcal{V}}_{\Delta} \leq -\Lambda_1 \mathcal{V}_{\Delta} + \frac{\delta_f^2}{2k_{\Delta}}$ provided $\zeta \in \mathcal{D}$. Therefore, $\mathcal{V}_{\Delta}(z(t)) \leq \mathcal{V}_{\Delta}(z(t_0)) e^{-\Lambda_1(t-t_0)} + \frac{\delta_f^2}{2k_{\Delta} \Lambda_1} (1 - e^{-\Lambda_1 t})$ and $\|z\| \leq \sqrt{\|z(t_0)\|^2 e^{-\Lambda_1(t-t_0)} + \frac{\delta_f^2}{k_{\Delta} \Lambda_1} (1 - e^{-\Lambda_1 t})}$, provided $\zeta \in \mathcal{D}$. For the prescribed accuracy δ_{Δ} , using the differential inequality, the settling time $t_{\Delta} = t_0 + \frac{1}{\Lambda_1} \ln \left(\frac{k_{\Delta} \Lambda_1 \|z(t_0)\|^2 - \delta_f^2}{k_{\Delta} \Lambda_1 \delta_{\Delta}^2 - \delta_f^2} \right)$ is obtained after imposing $\delta_{\Delta} \geq \sqrt{\|z(t_0)\|^2 e^{-\Lambda_1(t-t_0)} + \frac{\delta_f^2}{k_{\Delta} \Lambda_1} (1 - e^{-\Lambda_1 t})}$, provided $\zeta \in \mathcal{D}$. For the settling time to be feasible, the argument of the natural logarithm needs to be positive; imposing this condition yields the feasibility gain condition $k_{\Delta} \Lambda_1 > \frac{\delta_f^2}{\delta_{\Delta}^2}$. ■

Using Lemma 3, the observer errors, $\tilde{\Delta}$ and \tilde{r} will converge to the prescribed ultimate bound δ_{Δ} after the time t_{Δ} has passed.

IV. CL ADAPTATION LAWS FOR ADAPTIVE CONTROL

A. Weight Adaptation Law Algorithm 1

The first adaptation law is developed using traditional CL techniques guided by the output of the DNN. The shorthand notation $\Phi'(X, \hat{\theta})$ in (44) denotes the Jacobian of the DNN at the current state and weight estimates, and $\Phi'^{\top}(X_i, \hat{\theta})$ represents the Jacobian of the DNN using the current weight estimates and the previous state X_i , where $X_i \triangleq X(t_i)$ and $t_i \in [t_{\Delta}, t]$, represents states within this time interval. While some concurrent learning methods initialize the history stack at $t = 0$, in this approach, the history stack is only

constructed after the settling time (t_Δ defined in Lemma 3) has been reached. For the history stack to be accurate, this data is gathered after the observer errors have reached their ultimate bound. The implementable form of the CL-DNN update law is designed as

$$\dot{\hat{\theta}} = \text{proj} \left(\Gamma \left(\Phi'^\top(X, \hat{\theta})r - \gamma_1 \sum_{i=1}^N \Phi'^\top(X_i, \hat{\theta})(u_i - \hat{u}_i) - \gamma_2 \hat{\theta} \right) \right), \quad (44)$$

where $\gamma_1, \gamma_2 \in \mathbb{R}_{>0}$ denote user-selected adaptation gains, and $\Gamma \in \mathbb{R}^{\rho \times \rho}$ denotes a positive-definite time-varying least squares adaptation gain matrix

$$\frac{d}{dt} \Gamma^{-1} = \begin{cases} -\beta \Gamma^{-1} + \gamma_1 \left(\sum_{i=1}^N \Phi'^\top(X_i, \hat{\theta}) \Phi'(X_i, \hat{\theta}) \right), & \text{if } \lambda_{\Gamma, \min} < \lambda_{\min}(\Gamma) \text{ and } \lambda_{\max}(\Gamma) < \lambda_{\Gamma, \max} \\ 0, & \text{otherwise} \end{cases}, \quad (45)$$

where β represents a user selected forgetting factor $\beta : \mathbb{R}_{\geq 0} \rightarrow \mathbb{R}_{\geq 0}$, and $\lambda_{\Gamma, \min}, \lambda_{\Gamma, \max}$ are user-selected bounds for the minimum and maximum eigenvalues of Γ , respectively. The adaptation gain in (45) is initialized to be PD and it can be shown that $\Gamma(t)$ remains PD for all $t \in \mathbb{R}_{\geq 0}$ [45]. A reconstructed estimate of the calculated control input can be determined as

$$\hat{u}_i = \hat{\Delta}_i - \Phi(X_i, \hat{\theta}). \quad (46)$$

An analytical form of the implementable weight adaptation law in (44) can be obtained from (32), (33), (15), (44), and (46) as

$$\dot{\hat{\theta}} = \text{proj} \left(\Gamma \left(\Phi'^\top(X, \hat{\theta})r - \gamma_2 \hat{\theta} + \gamma_1 \sum_{i=1}^N \Phi'^\top(X_i, \hat{\theta}) \Phi'(X_i, \hat{\theta}) \hat{\theta} + \gamma_1 \sum_{i=1}^N \Phi'^\top(X_i, \hat{\theta}) \left(R(x, \tilde{\theta}) + \varepsilon(X_i) - \tilde{\Delta}_i \right) \right) \right). \quad (47)$$

B. Weight Adaptation Law Algorithm 2

The second weight adaptation law is developed to achieve parameter convergence and is based on the desire to leverage the internal dynamics of the DNN. The implementable form of the second CL-DNN update law is designed as

$$\dot{\hat{\theta}} = \text{proj} \left(\Gamma \left(\Phi'^\top(X, \hat{\theta})r - \gamma_2 \hat{\theta} - \gamma_1 \sum_{i=1}^N \Phi'^\top(X_i, \hat{\theta}) \left(u_i - \hat{\Delta}_i + \Phi'(X_i, \hat{\theta}) \hat{\theta} \right) \right) \right). \quad (48)$$

The analytical form of the weight adaptation law can be obtained by substituting (32), (33), and (15) into (48) which yields

$$\dot{\hat{\theta}} = \text{proj} \left(\Gamma \left(\Phi'^\top(X, \hat{\theta})r - \gamma_1 \sum_{i=1}^N \Phi'^\top(X_i, \hat{\theta}) \left(\tilde{\Delta}_i - \Phi(X_i, \hat{\theta}) - \Phi'(X_i, \hat{\theta}) \tilde{\theta} - R(X_i, \hat{\theta}) + \varepsilon(X_i) + \Phi'(X_i, \hat{\theta}) \hat{\theta} \right) - \gamma_2 \hat{\theta} \right) \right). \quad (49)$$

Based on the definition in (2), $\Phi(X, 0_\rho) = 0_n$. Using (20), (49), and canceling cross terms yields

$$\begin{aligned} \dot{\hat{\theta}} = \text{proj} & \left(\Gamma \left(\Phi'^\top(X, \hat{\theta})r + \gamma_1 \sum_{i=1}^N \Phi'^\top(X_i, \hat{\theta}) \Phi'(X_i, \hat{\theta}) \hat{\theta} \right. \right. \\ & \left. \left. - \gamma_1 \sum_{i=1}^N \Phi'^\top(X_i, \hat{\theta}) \left(\tilde{\Delta}_i + R(X_i, \hat{\theta}) - R(X_i, \tilde{\theta}) + \varepsilon(X_i) \right) \right. \right. \\ & \left. \left. - \gamma_2 \hat{\theta} \right) \right). \end{aligned} \quad (50)$$

The update laws developed in (44) and (48) are evaluated with their respective analytical forms in (47) and (50) and the controller developed in (38) in a Lyapunov-based stability analysis in the following section.

V. STABILITY ANALYSIS

Using (22), the following bound can be established

$$\|R(X, \tilde{\theta})\| \leq \rho_2(\|\zeta\|) \|\zeta\|^2 \quad (51)$$

where $\rho_2 : \mathbb{R}_{\geq 0} \rightarrow \mathbb{R}_{\geq 0}$ denotes a strictly-increasing function. Due to the fact that $R(X, \tilde{\theta})$, $\Phi'(X, \tilde{\theta})$, and ε are bounded, then the following bounds can be established

$$\begin{aligned} \|\Phi'^\top(X_i, \hat{\theta}) R(X_i, \tilde{\theta})\| & \leq \rho_3(\|\zeta_i\|) \|\zeta_i\|^2, \\ \|\Phi'^\top(X_i, \hat{\theta}) \varepsilon(X_i)\| & \leq \rho_4(\|X_i\|), \\ \|\Phi'^\top(X_i, \hat{\theta}) (\varepsilon(X_i) + R(X_i, \hat{\theta}))\| & \leq \rho_5(\|X_i\|), \end{aligned} \quad (52)$$

where $\rho_3, \rho_4, \rho_5 : \mathbb{R}_{\geq 0} \rightarrow \mathbb{R}_{\geq 0}$ denote strictly-increasing functions. Let $\rho_\Delta(\|\zeta\|) \geq \frac{1}{2} \rho_2^2(\|\zeta\|) \|\zeta\|^2 + \frac{\gamma_1}{2} \sum_{i=1}^N \rho_3^2(\|\zeta_i\|) \|\zeta_i\|^2$, $\rho_\delta(\|\zeta\|) \geq \frac{1}{2} \rho_1^2(\|\zeta\|) \|\zeta\|^2 + \frac{\gamma_1}{2} \sum_{i=1}^N \rho_3^2(\|\zeta_i\|) \|\zeta_i\|^2$, where $\rho_\Delta, \rho_\delta : \mathbb{R}_{\geq 0} \rightarrow \mathbb{R}_{\geq 0}$ denote invertible strictly-increasing functions. Since the approximation capabilities of DNNs holds on a compact domain Ω , the subsequent stability analysis requires ensuring $X(t) \in \Omega$ for all $t \in [t_0, \infty)$. This is achieved by yielding a stability result which constrains ζ in a compact domain. Therefore, consider the compact domains $\mathcal{D}_{3,4} \triangleq \{\sigma \in \mathbb{R}^\psi : \|\sigma\| \leq \chi_{3,4}\}$ in which ζ is supposed to lie to develop Theorem 3 and 4, respectively. It follows that if $\|\zeta\| \leq \chi_{3,4}$ then X can be bounded as $\|X\| \leq (\alpha + 2) \chi_{3,4} + \bar{x}_d + \dot{x}_d$. Therefore, select $\Omega_{3,4} \triangleq \{\sigma \in \mathbb{R}^{2n} : \|\sigma\| \leq (\alpha_1 + 2) \chi_{3,4} + \bar{x}_d + \dot{x}_d\}$. Then $\zeta \in \mathcal{D}_{3,4}$ implies $X \in \Omega_{3,4}$. Furthermore, to ensure that arbitrary initial conditions are always included, the user-selected constants χ_3 and χ_4 are selected as

$$\begin{aligned} \chi_3 & \triangleq \rho_\Delta^{-1}(\lambda_3 - \lambda_{3d}), \\ \chi_4 & \triangleq \rho_\delta^{-1}(\lambda_3 - \lambda_{3d}). \end{aligned} \quad (53)$$

Then it follows that $z(t_0) \in \mathcal{D}_{3,4} = \{\zeta \in \mathbb{R}^{2n+p} : \|\zeta\| \leq \chi\}$ is always satisfied. Because the solution $t \mapsto \zeta(t)$ is continuous², there exists a time-interval $\mathcal{I}_{1,2} \triangleq [t_0, t_1)$ such that $\|\zeta(t)\| < \mathcal{D}_{3,4}$ for all $t \in \mathcal{I}_{1,2}$. It follows that

²Continuous solutions exists over some time-interval for systems satisfying Caratheodory existence conditions. According to Caratheodory conditions for the system $\dot{y} = f(y, t)$, f should be locally bounded, continuous in y for each fixed t , measurable in t for each fixed y [46, Ch.2, Theorem 1.1]. The dynamics in \dot{z} satisfy the Caratheodory conditions.

$X(t) \in \Omega_{3,4}$ for all $t \in \mathcal{I}_{1,2}$, therefore the universal function approximation property holds over this time interval. In the subsequent stability analysis, we analyze the convergence properties of the solutions and also establish that $\mathcal{I}_{1,2}$ can be extended to $[t_0, \infty)$. Let $\lambda_3 \triangleq \min\{k_1 - 1, \alpha_1, \frac{\gamma_1}{2} \left(\lambda_{\min} \left\{ \sum_{i=1}^N \Phi'^\top(X_i, \hat{\theta}) \Phi'(X_i, \hat{\theta}) \right\} \right) + \frac{\gamma_2}{2} - \frac{\gamma_1 N \delta_\Delta}{2} + \gamma_1\}$, $\iota_3 \triangleq \frac{1}{2} \bar{\varepsilon}^2 + \frac{\gamma_2 \bar{\theta}^2}{2} + \frac{\gamma_1 N \delta_\Delta}{2} \sum_{i=1}^N \rho_1(\|X_i\|) - \frac{\gamma_1}{2} \sum_{i=1}^N (\rho_4(\|X_i\|))^2$ and $\iota_4 \triangleq \frac{1}{2} \bar{\varepsilon}^2 + \frac{\gamma_1 N \delta_\Delta}{2} \sum_{i=1}^N (\rho_1(\|X_i\|))^2 + \frac{\gamma_1}{2} \sum_{i=1}^N (\rho_5(\|X_i\|))^2 + \frac{\gamma_2}{2} \bar{\theta}^2$. Let the sets $\mathcal{S} \subset \mathcal{D}_3$ and $\mathcal{H} \subset \mathcal{D}_4$ be the sets of stabilizing initial conditions defined as

$$\mathcal{S} \triangleq \left\{ \sigma \in \mathbb{R}^\psi : \|\zeta(t_0)\| < \sqrt{\frac{\beta_1}{\beta_2} \rho_\Delta^{-1} (\lambda_3 - \lambda_{3d})^2 - \frac{\iota_3}{\lambda_{3d}}} \right\},$$

$$\mathcal{H} \triangleq \left\{ \sigma \in \mathbb{R}^\psi : \|\zeta(t_0)\| < \sqrt{\frac{\beta_1}{\beta_2} \rho_\Delta^{-1} (\lambda_3 - \lambda_{3d})^2 - \frac{\iota_4}{\lambda_{3d}}} \right\},$$

where $\lambda_{3d} \in \mathbb{R}_{\geq 0}$ denotes the desired convergence rate.

To guarantee that the adaptive update laws in Theorem 3 and Theorem 4 achieve the parameter identification objective described in (14), the history stack needs to be sufficiently rich, i.e., the system needs to be excited over a finite duration of time as specified in the following assumption.

Assumption 3. There exists $\lambda_e > 0$ and there exists $T > t_\Delta$ for all $t \geq T$ such that $\lambda_{\min} \left\{ \sum_{i=1}^N \Phi'^\top(X_i, \hat{\theta}) \Phi'(X_i, \hat{\theta}) \right\} \geq \lambda_e$.

To promote exploration of the parameter space, which is desirable to satisfy Assumption 2, the weights could be artificially excited as detailed in the following remark.

Remark 7. To promote exploration of the weights of the DNN, a user-selected time-varying bounded dither signal $d(t) : \mathbb{R}_{\geq 0} \rightarrow \mathbb{R}^\rho$ with the bound $\sup_{t \geq 0} \|d(t)\| \leq \bar{d}$ can be injected into the adaptation laws in (47) and (50). The resulting ι_3 and ι_4 would contain an additional term $\frac{\gamma_3}{2} \bar{d}^2$ where $\gamma_3 \in \mathbb{R}_{>0}$ is a user-selected gain.

Consider the Lyapunov candidate function $\mathcal{V} : \mathbb{R}^\psi \rightarrow \mathbb{R}_{\geq 0}$ defined as

$$\mathcal{V}(\zeta) = \frac{1}{2} r^\top r + \frac{1}{2} e^\top e + \frac{1}{2} \tilde{\theta}^\top \Gamma^{-1} \tilde{\theta}, \quad (54)$$

which satisfies the inequality

$$\beta_1 \|\zeta\|^2 \leq \mathcal{V}(\zeta) \leq \beta_2 \|\zeta\|^2 \quad (55)$$

where $\beta_1 \triangleq \min \left\{ \frac{1}{2}, \frac{1}{2}, \frac{1}{2} \frac{1}{\lambda_{\Gamma, \max}} \right\}$ and $\beta_2 \triangleq \max \left\{ \frac{1}{2}, \frac{1}{2}, \frac{1}{2} \frac{1}{\lambda_{\Gamma, \min}} \right\}$. Taking the time derivative of $\mathcal{V}(\zeta)$, and applying (35) and (39) yields

$$\dot{\mathcal{V}} = r^\top \left(\Phi'(X, \hat{\theta}) \tilde{\theta} + R(X, \tilde{\theta}) + \varepsilon(X) - k_1 r - e \right) - e^\top \alpha_1 e + \tilde{\theta}^\top \Gamma^{-1} \dot{\tilde{\theta}} + \frac{1}{2} \tilde{\theta}^\top \left(\frac{d}{dt} \Gamma^{-1} \right) \tilde{\theta}. \quad (56)$$

Using (45), the last term in (56) can be bounded as

$$\frac{1}{2} \tilde{\theta}^\top \left(\frac{d}{dt} \Gamma^{-1} \right) \tilde{\theta} \leq \frac{1}{2} \tilde{\theta}^\top \gamma_1 \left(\sum_{i=1}^N \Phi'^\top(X_i, \hat{\theta}) \Phi'(X_i, \hat{\theta}) \right) \tilde{\theta}. \quad (57)$$

Theorem 3 and Theorem 4 provide convergence guarantees for the tracking and parameter estimation errors using the update laws in (47) and (50), respectively.

Theorem 3. Let the gain conditions $k_\Delta \Lambda_1 > \frac{\delta_f^2}{\delta_\Delta^2}$ and $\lambda_{3d} > 0$ be satisfied, and $\|\zeta(0)\| \in \mathcal{S}$. For the dynamical system in (32), the controller in (38) and the adaptation law developed in (47) ensures the concatenated error vector ζ is bounded in the sense that $\|\zeta(t)\| \leq \sqrt{\frac{\beta_2}{\beta_1} \|\zeta(t_0)\|^2 e^{-\frac{\lambda_{3d}}{\beta_2} (t-t_0)} + \frac{\beta_2 \iota_3}{\beta_1 \lambda_{3d}} \left(1 - e^{-\frac{\lambda_{3d}}{\beta_2} t} \right)}$, for all $t \in \mathbb{R}_{\geq 0}$.

Proof: Consider the candidate Lyapunov function in (54). From (47), (56), and using (57), $\dot{\mathcal{V}}$ can be upper bounded as

$$\begin{aligned} \dot{\mathcal{V}} \leq & -r^\top k_1 r - e^\top \alpha_1 e + r^\top \left(R(X, \tilde{\theta}) + \varepsilon(X) \right) \\ & - \tilde{\theta}^\top \frac{\gamma_1}{2} \sum_{i=1}^N \Phi'^\top(X_i, \hat{\theta}) \Phi'(X_i, \hat{\theta}) \tilde{\theta} - \tilde{\theta}^\top \gamma_2 \tilde{\theta} \\ & - \tilde{\theta}^\top \gamma_1 \sum_{i=1}^N \Phi'^\top(X_i, \hat{\theta}) \left(R(X_i, \tilde{\theta}) + \varepsilon(X_i) - \tilde{\Delta}_i \right) \\ & + \tilde{\theta}^\top \gamma_2 \theta^*. \end{aligned} \quad (58)$$

Using Lemma 3, the bound $\|\tilde{\Delta}_i\| \leq \delta_\Delta$ holds for all $i \in \{1, \dots, N\}$, provided $\zeta \in \mathcal{D}_3$, the data is collected after the settling time t_Δ , and the feasibility gain condition $k_\Delta \Lambda_1 > \frac{\delta_f^2}{\delta_\Delta^2}$ is satisfied. Therefore, using the bounds in (51) and (52), $\dot{\mathcal{V}}$ can be upper bounded as

$$\dot{\mathcal{V}} \leq -(\lambda_3 - \rho_\Delta(\|\zeta\|)) \|\zeta\|^2 + \iota_3, \quad (59)$$

when $\zeta \in \mathcal{D}_3$. Therefore, when ζ is initialized such that $\zeta(t_0) \in \mathcal{S}$, then it follows that $\lambda_3 > \lambda_{3d} + \rho_\Delta \left(\sqrt{\frac{\beta_2}{\beta_1} \|\zeta(t_0)\|^2} + \frac{\beta_2 \iota_3}{\beta_1 \lambda_{3d}} \right)$. Recall that, because the solution $t \mapsto \zeta(t)$ is continuous, ζ cannot instantaneously escape \mathcal{S} at t_0 , therefore there exists a time-interval \mathcal{I}_1 such that $\zeta(t) \in \mathcal{S}$ for all $t \in \mathcal{I}_1$, implying

$$\|\zeta(t)\| < \sqrt{\frac{\beta_2}{\beta_1} \|\zeta(t_0)\|^2 + \frac{\beta_2 \iota_3}{\beta_1 \lambda_{3d}}} \quad (60)$$

for all $t \in \mathcal{I}_1$. Because ρ_Δ is strictly increasing, $\rho_\Delta(\|\zeta(t)\|) < \rho_\Delta \left(\sqrt{\frac{\beta_2}{\beta_1} \|\zeta(t_0)\|^2 + \frac{\beta_2 \iota_3}{\beta_1 \lambda_{3d}}} \right)$ for all $t \in \mathcal{I}_1$. As a result,

$$\dot{\mathcal{V}} \leq -\lambda_{3d} \|\zeta\|^2 + \iota_3 \quad (61)$$

for all $t \in \mathcal{I}_1$. Using (55), $\dot{\mathcal{V}}$ and solving the differential inequality over \mathcal{I}_1 yields $\mathcal{V}(\zeta(t)) \leq \mathcal{V}(\zeta(t_0)) e^{-\frac{\lambda_{3d}}{\beta_2} (t-t_0)} + \frac{\beta_2 \iota_3}{\lambda_{3d}} \left(1 - e^{-\frac{\lambda_{3d}}{\beta_2} t} \right)$. It remains to be shown that \mathcal{I}_1 can be extended to $[t_0, \infty)$. Assume for the sake of contradiction that \mathcal{I}_1 has to be bounded, i.e., t_1 has

to be finite. Equivalently, there exists t_1 for which there does not exist $t_2 > t_1$ such that $\|\zeta(t)\| < \sqrt{\frac{\beta_2}{\beta_1} \|\zeta(t_0)\|^2 + \frac{\beta_2 \iota_3}{\beta_1 \lambda_{3d}}}$ for all $t \in [t_1, t_2]$. Substituting $t = t_1$ into (60) yields $\|\zeta(t_1)\| < \sqrt{\frac{\beta_2}{\beta_1} \|\zeta(t_0)\|^2 + \frac{\beta_2 \iota_3}{\beta_1 \lambda_{3d}}}$. Hence, because the solution $t \mapsto \zeta(t)$ is continuous, for every t_1 there exists a $t_2 > t_1$ such that $\|\zeta(t)\| < \sqrt{\frac{\beta_2}{\beta_1} \|\zeta(t_0)\|^2 + \frac{\beta_2 \iota_3}{\beta_1 \lambda_{3d}}}$ for all $t \in [t_1, t_2]$, violating the assumption made by contradiction. Therefore, \mathcal{I}_1 can be extended to the interval $[t_0, \infty)$ and $\|\zeta(t)\| < \sqrt{\frac{\beta_2}{\beta_1} \|\zeta(t_0)\|^2 + \frac{\beta_2 \iota_3}{\beta_1 \lambda_{3d}}}$ for all $t \in [t_0, \infty)$. Then, [44, Def. 4.6] can be invoked to conclude that ζ is bounded such that $\|\zeta(t)\| \leq \sqrt{\frac{\beta_2}{\beta_1} \|\zeta(t_0)\|^2 e^{-\frac{\lambda_{3d}}{\beta_2}(t-t_0)} + \frac{\beta_2 \iota_3}{\beta_1 \lambda_{3d}} \left(1 - e^{-\frac{\lambda_{3d}}{\beta_2}t}\right)}$. Hence, solving the differential inequality in (61) and upperbounding yields that if $\zeta(t_0) \in \mathcal{S}$, then $\zeta(t) \in \mathcal{S} \subset \mathcal{D}_3$ and therefore $X \in \Omega_3$ for all $t \geq 0$. Using (54) and (61) implies $e, r, \tilde{\theta} \in \mathcal{L}_\infty$. The fact that $x_d, \dot{x}_d, \ddot{x}_d, e, r \in \mathcal{L}_\infty$ implies $x, \dot{x} \in \mathcal{L}_\infty$, using this and the fact $\tilde{\theta} \in \mathcal{L}_\infty$ is bounded by the use of the projection operator implies u is bounded. ■

Theorem 4. *Let the gain conditions $k_\Delta \Lambda_1 > \frac{\delta_f^2}{\delta_\Delta^2}$ and $\lambda_{3d} > 0$ be satisfied, and $\|\zeta(0)\| \in \mathcal{H}$. For the dynamical system in (32), the controller in (38), the adaptation law developed in (50) ensures the concatenated error vector ζ is bounded in the sense that $\|\zeta(t)\| \leq \sqrt{\frac{\beta_2}{\beta_1} \|\zeta(t_0)\|^2 e^{-\frac{\lambda_{3d}}{\beta_2}(t-t_0)} + \frac{\beta_2 \iota_4}{\beta_1 \lambda_{3d}} \left(1 - e^{-\frac{\lambda_{3d}}{\beta_2}t}\right)}$, for all $t \in \mathbb{R}_{\geq 0}$.*

Proof: Consider the candidate Lyapunov function in (54). Then using (56), applying (50), the definition for $\tilde{\theta}$, and using (57), $\dot{\mathcal{V}}$ can be upper bounded as

$$\begin{aligned} \dot{\mathcal{V}} &\leq -r^\top k_1 r - e^\top \alpha_1 e + r^\top \left(R(X_i, \tilde{\theta}) + \varepsilon(X) \right) \\ &\quad - \tilde{\theta}^\top \gamma_1 \left(\frac{1}{2} \sum_{i=1}^N \Phi'^\top(X_i, \hat{\theta}) \Phi'(X_i, \hat{\theta}) \tilde{\theta} \right. \\ &\quad \left. - \sum_{i=1}^N \Phi'^\top(X_i, \hat{\theta}) \left(\tilde{\Delta}_i + R(X_i, \hat{\theta}) - R(X_i, \tilde{\theta}) + \varepsilon(X_i) \right) \right) \\ &\quad + \tilde{\theta}^\top \gamma_2 \theta^* - \tilde{\theta}^\top \gamma_2 \tilde{\theta}. \end{aligned} \quad (62)$$

Using Lemma 3, the bound $\|\tilde{\Delta}_i\| \leq \delta_\Delta$ holds for all $i \in \{1, \dots, N\}$, provided $\zeta \in \mathcal{D}_4$, the data is collected after the settling time t_Δ , and the feasibility gain condition $k_\Delta \Lambda_1 > \frac{\delta_f^2}{\delta_\Delta^2}$ is satisfied. Therefore, using the bounds in (51) and (52), $\dot{\mathcal{V}}$ can be upper bounded as

$$\dot{\mathcal{V}} \leq -(\lambda_3 - \rho_\delta(\|\delta\|)) + \iota_4, \quad (63)$$

when $\zeta \in \mathcal{D}_4$. Therefore, when ζ is initialized such that $\zeta(t_0) \in \mathcal{H}$, then it follows that $\lambda_3 > \lambda_{3d} + \rho_\delta \left(\sqrt{\frac{\beta_2}{\beta_1} \|\zeta(t_0)\|^2 + \frac{\beta_2 \iota_4}{\beta_1 \lambda_{3d}}} \right)$. Recall that, because the solution $t \mapsto \zeta(t)$ is continuous, ζ cannot instantaneously escape \mathcal{H} at t_0 , therefore there exists a time-interval \mathcal{I}_2 such that $\zeta(t) \in \mathcal{H}$ for all $t \in \mathcal{I}_2$, implying

$$\|\zeta(t)\| < \sqrt{\frac{\beta_2}{\beta_1} \|\zeta(t_0)\|^2 + \frac{\beta_2 \iota_4}{\beta_1 \lambda_{3d}}} \quad (64)$$

for all $t \in \mathcal{I}_2$. Because ρ_δ is strictly increasing, $\rho_\delta(\|\zeta(t)\|) < \rho_\delta \left(\sqrt{\frac{\beta_2}{\beta_1} \|\zeta(t_0)\|^2 + \frac{\beta_2 \iota_4}{\beta_1 \lambda_{3d}}} \right)$ for all $t \in \mathcal{I}_2$. As a result,

$$\dot{\mathcal{V}} \leq -\lambda_{3d} \|\zeta\|^2 + \iota_4 \quad (65)$$

for all $t \in \mathcal{I}_2$. Using (55), $\dot{\mathcal{V}}$ and solving the differential inequality over \mathcal{I}_2 yields $\mathcal{V}(\zeta(t)) \leq \mathcal{V}(\zeta(t_0)) e^{-\frac{\lambda_{3d}}{\beta_2}(t-t_0)} + \frac{\beta_2 \iota_4}{\beta_1 \lambda_{3d}} \left(1 - e^{-\frac{\lambda_{3d}}{\beta_2}t}\right)$. Using the same process as Theorem 3 it can be shown that \mathcal{I}_2 can be extended to the interval $[t_0, \infty)$ and $\|\zeta(t)\| < \sqrt{\frac{\beta_2}{\beta_1} \|\zeta(t_0)\|^2 + \frac{\beta_2 \iota_4}{\beta_1 \lambda_{3d}}}$ for all $t \in [t_0, \infty)$. Then, [44, Def. 4.6] can be invoked to conclude that ζ is bounded such that $\|\zeta(t)\| \leq \sqrt{\frac{\beta_2}{\beta_1} \|\zeta(t_0)\|^2 e^{-\frac{\lambda_{3d}}{\beta_2}(t-t_0)} + \frac{\beta_2 \iota_4}{\beta_1 \lambda_{3d}} \left(1 - e^{-\frac{\lambda_{3d}}{\beta_2}t}\right)}$. Therefore, if $\zeta(t_0) \in \mathcal{H}$, then $\zeta(t) \in \mathcal{H} \subset \mathcal{D}_4$ and therefore $X \in \Omega_4$ for all $t \geq 0$. Using (54) and (65) implies $e, r, \tilde{\theta} \in \mathcal{L}_\infty$. The fact that $x_d, \dot{x}_d, \ddot{x}_d, e, r \in \mathcal{L}_\infty$ implies $x, \dot{x} \in \mathcal{L}_\infty$, using this and the fact $\tilde{\theta} \in \mathcal{L}_\infty$ is bounded by the use of the projection operator implies u is bounded. ■

VI. SIMULATIONS

Simulation results are provided to demonstrate the performance of the developed method and comparisons are provided using the implementable forms of the updates proposed in (47) and (50) as outlined in (44) and (48) as well as the baseline method outlined in [3]. To demonstrate the performance improvement and applicability of the developed method across a variety of nonlinear systems, simulations were performed on two unknown nonlinear systems modeled by (32) with different models for $f(x, \dot{x})$ given by $f_1(x, \dot{x}) = \begin{bmatrix} \sin(x_1 + x_2) \cos(\dot{x}_1 - \dot{x}_2) + \cos(x_1) \sin(x_2) \cos(\dot{x}_1) \sin(\dot{x}_2) \\ \cos(x_1) \sin(x_2) \cos(\dot{x}_1) \sin(\dot{x}_2) - \sin(x_1 + x_2) \cos(\dot{x}_1 - \dot{x}_2) \sin(x_1) \end{bmatrix}$ [N] and $f_2(x, \dot{x}) = \begin{bmatrix} x_1 \dot{x}_2 \tanh(x_2) + \operatorname{sech}^2(x_1) \\ \operatorname{sech}^2(\dot{x}_1 + \dot{x}_2) - \operatorname{sech}^2(x_2) \end{bmatrix}$ [N], respectively. Simulations were run for 100s with an update preformed every 0.01s to demonstrate the impact of the real-time adaptation. The settling time t_Δ was selected as 3s and the history stack was constructed using a sliding window of the previous 200 data points (2s of data) with the stack being updated every 5 new data points gathered or 0.05s. The tracking objective was preformed using two trajectory formulations, the first was a circular desired trajectory selected as $q_d = \begin{bmatrix} 0.7 \cos\left(\frac{\pi}{4}t\right) \\ 0.7 \sin\left(\frac{\pi}{4}t\right) \end{bmatrix} \in \mathbb{R}^2$ [rad] and a sinusoidal desired trajectory selected as $q_d = \begin{bmatrix} 0.7 \sin\left(\frac{\pi}{4}t\right) \\ \frac{\pi}{4} \sin\left(\frac{\pi}{4}t\right) \end{bmatrix} \in \mathbb{R}^2$ [rad]. The simulation is initialized at $q(0) = [1.0472, -0.5236]^\top$ [rad] and $\dot{q}(0) = [0, 0]$ [rad/s]. To promote exploration of the weights, an artificial disturbance described as $d(t) = \cos^2(0.2t) + \sin^2(2t) \cos(0.1t) + \sin^2(-1.2t) \cos(0.5t) + \sin^2(t)$ was added to the update law as described in Remark 7. The DNNs are composed of 4 layers, 2 neurons, and tanh activation functions. The weights of the DNN were randomly initialized from a uniform distribution $U(-1, 1)$. The gains were selected as $\alpha_1 = 15$, $\alpha_2 = 50$, $k_1 = 40$, $k_\Delta = 20$, $\beta = 0.01$, $\gamma_1 = 0.12$, $\gamma_2 = 0.005$, $\gamma_3 = 0.001$,

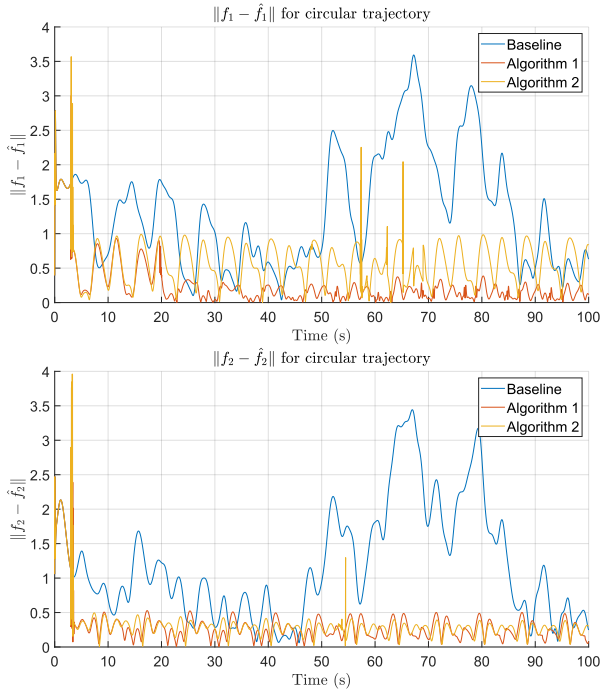


Figure 1. Function approximation error $\|f(x, \dot{x}) - \hat{f}(x, \dot{x})\|$ for circular trajectory and f_1 and f_2 dynamics

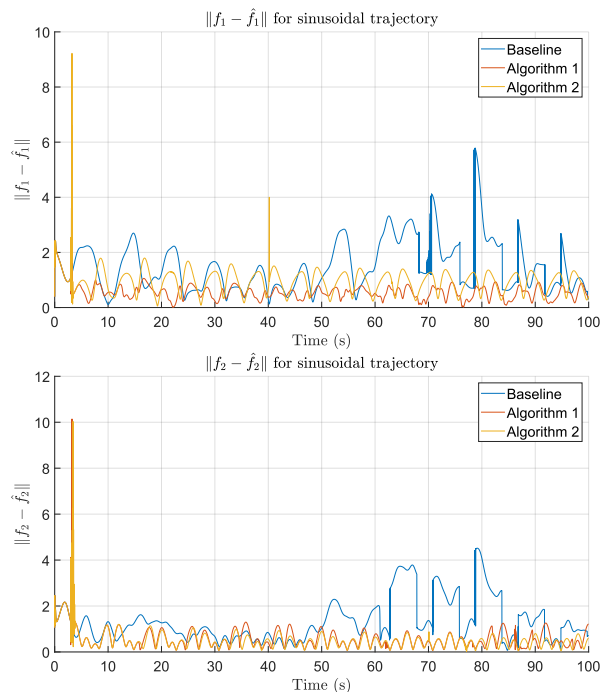


Figure 2. $\|f(x, \dot{x}) - \hat{f}(x, \dot{x})\|$ for Sinusoidal trajectory and f_1 and f_2 dynamics

$\Gamma(0) = 1$. The same randomly selected initial weights and control gains were used for all architectures and trajectory types to demonstrate the performance of the adaptation under the same conditions. For the baseline method the gain associated with the history stack in the update law γ_1 , and the sigma-modification technique γ_2 , were set to be 0. Both algorithms satisfy the FE condition stated in Assumption 2 a minimum of once during the simulation run time for the circular trajectory. For the sinusoidal trajectory, Algorithm 1 meets the FE condition while Algorithm 2 does not, however as shown in Table II there is empirically a significant performance improvement in function approximation error both on and off the trajectory compared to the baseline from incorporating previously seen data in the adaptation law.

The root mean squared (RMS) tracking error for Algorithm 1, Algorithm 2, and the baseline method are tabulated in Tables I and II and demonstrated that all methods yielded similar tracking error performance and required control effort. The similarity in tracking error performance is expected due to the powerful function approximation capabilities of DNNs. However, the developed adaptation laws are motivated by the parameter identification objective, therefore it is expected to see an improvement in the error between the actual function and the estimated function which can be quantified as $f(x, \dot{x}) - \hat{f}(x, \dot{x})$. This error is quantified in Tables I and II and shown in Figures 1 and 2 indicates that the use of the developed update laws result in function approximation performance beyond being able to compensate for the unknown dynamics and demonstrates between a 40.5% and 73.6% improvement in identifying the true function for multiple types of dynamics and trajectories compared to a method which does not use the CL-based update law. To evaluate the performance of the DNN from off-trajectory data, a test data set involving 100 data points with values selected from the distribution $U(-1, 1)$ is constructed. The function evaluated at these points is denoted $f(x_{OT}, \dot{x}_{OT})$ and the estimate at these points is denoted $\hat{f}(x_{OT}, \dot{x}_{OT})$. The mean function approximation error for the off-trajectory points is shown in Figures 3 and 4 demonstrating improved function approximation capabilities on unseen data for Algorithm 1 and Algorithm 2 compared to the baseline. Similarly, these capabilities are used as a metric in Tables I and II to demonstrate the performance improvement resulting in between 58.88% and 74.75% improvement in off-trajectory function approximation compared to the baseline method.

VII. CONCLUSIONS

An adaptive CL-DNN-based controller was developed for a control-affine general nonlinear system. Leveraging previously gathered data to form a history-stack, the developed Lb-CL adaptation is capable of achieving both tracking error and parameter estimation error convergence. A Lyapunov-based stability analysis guarantees ultimately bounded error convergence for both the tracking and the weight estimation errors. Simulations were conducted on two distinct nonlinear systems using two different trajectories, all under

Table I
TRACKING AND CONTROL EFFORT METRICS FOR THE DEVELOPED METHODS VS. BASELINE METHOD FOR CIRCULAR TRAJECTORY

	Algorithm 1		Circular Trajectory Algorithm 2		Baseline	
	f_1	f_2	f_1	f_2	f_1	f_2
RMS $\ e\ $	0.0144 [rad]	0.0144 [rad]	0.0144 [rad]	0.0144 [rad]	0.0146 [rad]	0.0146 [rad]
% Improvement over Baseline	1.461%	1.273%	1.307%	1.265%	-	-
RMS $\ \tau\ $	4.640 [N]	4.655 [N]	4.641 [N]	4.656 [N]	4.639 [N]	4.654 [N]
% Improvement over Baseline	-0.0099%	-0.0215%	-0.0343%	-0.0428%	-	-
RMS $\ f(x, \dot{x}) - \hat{f}(x, \dot{x})\ $	0.4121 [N]	0.4269 [N]	0.6860 [N]	0.4411 [N]	1.562 [N]	1.453 [N]
% Improvement over Baseline	73.62%	70.66%	56.09%	69.64%	-	-
RMS $\ f(x_{OT}, \dot{x}_{OT}) - \hat{f}(x_{OT}, \dot{x}_{OT})\ $	0.3518 [N]	0.3232 [N]	0.4293 [N]	0.3603 [N]	1.548 [N]	1.439 [N]
% Improvement over Baseline	73.86%	74.75%	68.10%	71.85%	-	-

Table II
TRACKING AND CONTROL EFFORT METRICS FOR THE DEVELOPED METHODS VS. BASELINE METHOD FOR SINUSOIDAL TRAJECTORY

	Algorithm 1		Sinusoidal Trajectory Algorithm 2		Baseline	
	f_1	f_2	f_1	f_2	f_1	f_2
RMS $\ e\ $	0.0268 [rad]	0.0268 [rad]	0.0268 [rad]	0.0268 [rad]	0.0269 [rad]	0.0269 [rad]
% Improvement over Baseline	0.5408%	0.4217%	0.3816%	0.4205%	-	-
RMS $\ \tau\ $	7.959 [N]	7.927 [N]	7.961 [N]	7.928 [N]	7.962 [N]	7.926 [N]
% Improvement over Baseline	0.0347%	-0.0116%	0.0098%	-0.0226%	-	-
RMS $\ f(x, \dot{x}) - \hat{f}(x, \dot{x})\ $	0.6210 [N]	0.7188 [N]	1.038 [N]	0.6577 [N]	1.744 [N]	1.611 [N]
% Improvement over Baseline	64.38%	55.39%	40.46%	59.19%	-	-
RMS $\ f(x_{OT}, \dot{x}_{OT})\ $	0.4315 [N]	0.4878 [N]	0.5515 [N]	0.4496 [N]	1.759 [N]	1.624 [N]
% Improvement over Baseline	67.83%	64.69%	58.88%	67.46%	-	-

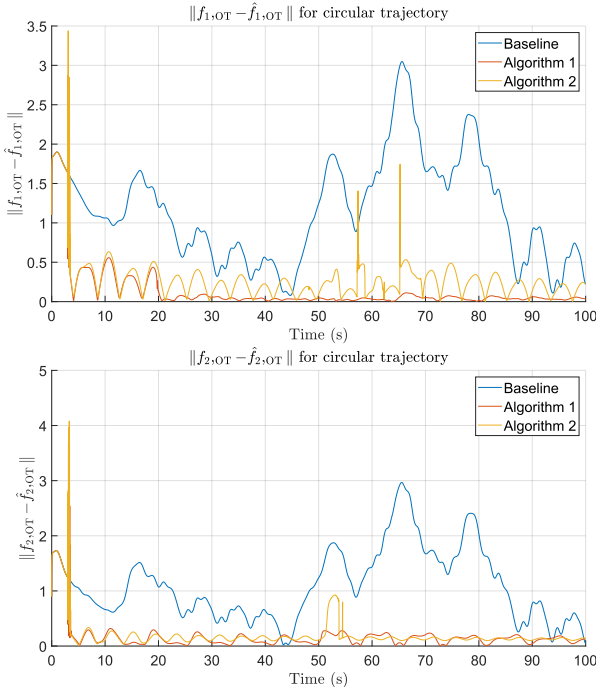


Figure 3. $\|f(x_{OT}, \dot{x}_{OT}) - \hat{f}(x_{OT}, \dot{x}_{OT})\|$ for Circular trajectory and f_1 and f_2 dynamics

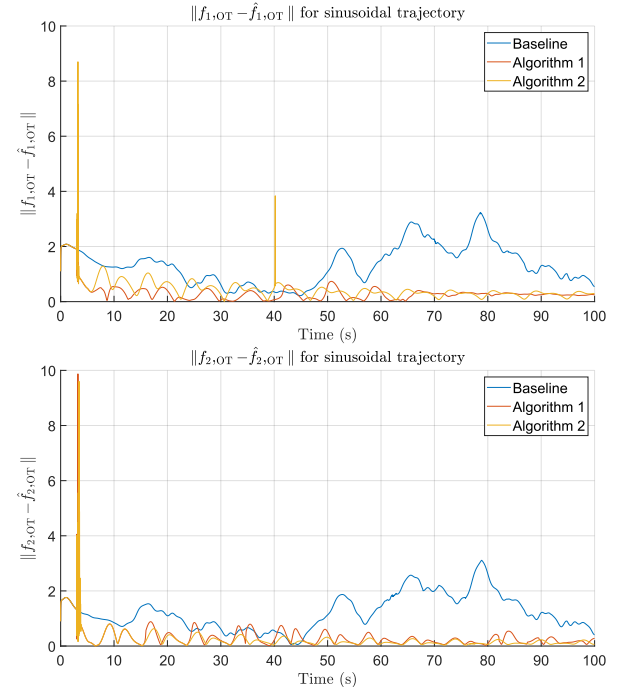


Figure 4. $\|f(x_{OT}, \dot{x}_{OT}) - \hat{f}(x_{OT}, \dot{x}_{OT})\|$ for Circular trajectory and f_1 and f_2 dynamics

the same initial conditions and control gains. The system identification objective showed improvements ranging from 40.5% to 73.6% compared to the baseline method while providing similar tracking error performance and control effort. Similarly, off-trajectory simulations demonstrated consistent performance gains, with improvements of 58.88% and

74.75% for the developed methods, highlighting their robust effectiveness across different systems.

REFERENCES

[1] R. Sun, M. Greene, D. Le, Z. Bell, G. Chowdhary, and W. E. Dixon, “Lyapunov-based real-time and iterative adjustment of deep neural networks,” *IEEE Control Syst. Lett.*, vol. 6, pp. 193–198, 2022.

[2] G. Joshi, J. Virdi, and G. Chowdhary, "Design and flight evaluation of deep model reference adaptive controller," in *AIAA Scitech 2020 Forum*, p. 1336, 2020.

[3] O. Patil, D. Le, M. Greene, and W. E. Dixon, "Lyapunov-derived control and adaptive update laws for inner and outer layer weights of a deep neural network," *IEEE Control Syst Lett.*, vol. 6, pp. 1855–1860, 2022.

[4] O. S. Patil, E. J. Griffis, W. A. Makumi, and W. E. Dixon, "Composite adaptive Lyapunov-based deep neural network (Lb-DNN) controller," *arXiv preprint arXiv:1306.3432*, 2023.

[5] H. M. Sweatland, O. S. Patil, and W. E. Dixon, "Adaptive deep neural network-based control barrier functions," *arXiv preprint arXiv:2406.14430*, 2025.

[6] S. Basyal, J. Ting, K. Mishra, and B. C. Allen, "Augmentation of a Lyapunov-based deep neural network controller with concurrent learning for control-affine nonlinear systems," *Proc. Am. Control Conf.*, pp. 2870–2875, 2024.

[7] R. Hart, E. Griffis, O. Patil, and W. E. Dixon, "Lyapunov-based physics-informed long short-term memory (LSTM) neural network-based adaptive control," *IEEE Control Syst. Lett.*, vol. 8, pp. 13–18, 2024.

[8] E. Griffis, O. Patil, Z. Bell, and W. E. Dixon, "Lyapunov-based long short-term memory (Lb-LSTM) neural network-based control," *IEEE Control Syst. Lett.*, vol. 7, pp. 2976–2981, 2023.

[9] G. Shi, X. Shi, M. O'Connell, R. Yu, K. Azizzadenesheli, A. Anandkumar, Y. Yue, and S.-J. Chung, "Neural lander: Stable drone landing control using learned dynamics," in *Proc. IEEE Int. Conf. Robot. Autom.*, pp. 9784–9790, 2019.

[10] A. Punjani and P. Abbeel, "Deep learning helicopter dynamics models," in *Proc. IEEE Int. Conf. Robot. Autom.*, pp. 3223–3230, 2015.

[11] S. Bansal, A. K. Akametalu, F. J. Jiang, F. Laine, and C. J. Tomlin, "Learning quadrotor dynamics using neural network for flight control," in *Proc. IEEE Conf. Decis. Control*, pp. 4653–4660, 2016.

[12] Q. Li, J. Qian, Z. Zhu, X. Bao, M. K. Helwa, and A. P. Schoellig, "Deep neural networks for improved, impromptu trajectory tracking of quadrotors," in *Proc. IEEE Int. Conf. Robot. Autom.*, pp. 5183–5189, 2017.

[13] B. Karg and S. Lucia, "Efficient representation and approximation of model predictive control laws via deep learning," *IEEE Trans. Cybern.*, vol. 50, no. 9, pp. 3866–3878, 2020.

[14] R. Hart, O. Patil, E. Griffis, and W. E. Dixon, "Deep Lyapunov-based physics-informed neural networks (DeLb-PINN) for adaptive control design," in *Proc. IEEE Conf. Decis. Control*, pp. 1511–1516, 2023.

[15] D. M. Le, O. S. Patil, C. Nino, and W. E. Dixon, "Accelerated gradient approach for neural network-based adaptive control of nonlinear systems," in *Proc. IEEE Conf. Decis. Control*, pp. 3475–3480, 2022.

[16] C. F. Nino, O. S. Patil, J. Philor, Z. Bell, and W. E. Dixon, "Deep adaptive indirect herding of multiple target agents with unknown interaction dynamics," in *Proc. IEEE Conf. Decis. Control*, pp. 2509–2514, 2023.

[17] H. Lu, J. Wu, and W. Wang, "Adaptive deep neural network optimized control for a class of nonlinear strict-feedback systems with prescribed performance," *Int. J. Adapt. Control Signal Process.*, pp. 1–24, 2024.

[18] J. Mei, H. Jian, Y. Li, W. Wang, and D. Lin, "Deep neural networks-based output-dependent intermittent control for a class of uncertain nonlinear systems," *Chaos Solitons Fractals*, vol. 185, p. 114999, 2024.

[19] A. Pulido, K. Volle, K. Waters, Z. I. Bell, P. Ganesh, and J. Shin, "Uncertainty-aware guidance for target tracking subject to intermittent measurements using motion model learning," *arXiv preprint arXiv:2402.00671*, 2024.

[20] Y. Pan and H. Yu, "Composite learning robot control with guaranteed parameter convergence," *Automatica*, vol. 89, pp. 415–419, Mar. 2018.

[21] G. Chowdhary, M. Mühlegg, J. How, and F. Holzapfel, "Concurrent learning adaptive model predictive control," in *Advances in Aerospace Guidance, Navigation and Control*, pp. 29–47, Springer Berlin Heidelberg, 2013.

[22] A. Parikh, R. Kamalapurkar, and W. E. Dixon, "Integral concurrent learning: Adaptive control with parameter convergence using finite excitation," *Int J Adapt Control Signal Process.*, vol. 33, pp. 1775–1787, Dec. 2019.

[23] R. Kamalapurkar, B. Reish, G. Chowdhary, and W. E. Dixon, "Concurrent learning for parameter estimation using dynamic state-derivative estimators," *IEEE Trans. Autom. Control*, vol. 62, pp. 3594–3601, July 2017.

[24] S. B. Roy, S. Bhasin, and I. N. Kar, "Combined MRAC for unknown MIMO LTI systems with parameter convergence," *IEEE Trans. Autom. Control*, vol. 63, pp. 283–290, Jan. 2018.

[25] R. Ortega, S. Aranovskiy, A. A. Pyrkin, A. Astolfi, and A. A. Bobtsov, "New results on parameter estimation via dynamic regressor extension and mixing: Continuous and discrete-time cases," *IEEE Trans. Autom. Control*, vol. 66, no. 5, pp. 2265–2272, 2021.

[26] C. Cao, A. M. Annaswamy, and A. Kojic, "Parameter convergence in nonlinearly parameterized systems," *IEEE Trans. Autom. Control*, vol. 48, no. 3, pp. 397–412, 2003.

[27] L. Wang, R. Ortega, A. Bobtsov, J. G. Romero, and B. Yi, "Identifiability implies robust, globally exponentially convergent on-line parameter estimation: Application to model reference adaptive control," *arXiv preprint arXiv:2108.08436*, 2021.

[28] R. Ortega, A. Bobtsov, N. Nikolaev, and R. Costa-Castelló, "Parameter estimation of two classes of nonlinear systems with non-separable nonlinear parameterizations," *Automatica*, vol. 163, p. 111559, 2024.

[29] D. Rolnick and M. Tegmark, "The power of deeper networks for expressing natural functions," in *Int. Conf. Learn. Represent.*, 2018.

[30] O. S. Patil, D. M. Le, E. Griffis, and W. E. Dixon, "Deep residual neural network (ResNet)-based adaptive control: A Lyapunov-based approach," in *Proc. IEEE Conf. Decis. Control*, pp. 3487–3492, 2022.

[31] P. Kidger and T. Lyons, "Universal approximation with deep narrow networks," in *Conf. Learn. Theory*, pp. 2306–2327, 2020.

[32] I. Goodfellow, Y. Bengio, and A. Courville, *Deep Learning*, vol. 1. MIT Press, 2016.

[33] K. Kawaguchi and Y. Bengio, "Depth with nonlinearity creates no bad local minima in ResNets," *Neural Netw.*, vol. 118, pp. 167–174, 2019.

[34] K. Kawaguchi, "Deep learning without poor local minima," *NeurIPS*, vol. 29, 2016.

[35] H. Lu and K. Kawaguchi, "Depth creates no bad local minima," *arXiv preprint arXiv:1702.08580*, 2017.

[36] S. Du, J. Lee, Y. Tian, A. Singh, and B. Poczos, "Gradient descent learns one-hidden-layer CNN: Dont be afraid of spurious local minima," in *Proc. 35th Int. Conf. Mach. Learn.*, vol. 80, pp. 1339–1348, 2018.

[37] M. Grewal and K. Glover, "Identifiability of linear and nonlinear dynamical systems," *IEEE Trans. Autom. Control*, vol. 21, no. 6, pp. 833–837, 1976.

[38] S. Boyd and L. Vandenberghe, *Convex Optimization*. New York, NY, USA: Cambridge University Press, 2004.

[39] S. Friedberg, A. Insel, and L. Spence, *Linear Algebra*, vol. 4. 2003.

[40] M. Krstic, I. Kanellakopoulos, and P. V. Kokotovic, *Nonlinear and Adaptive Control Design*. New York: John Wiley & Sons, 1995.

[41] O. S. Patil, B. C. Fallin, C. F. Nino, R. G. Hart, and W. E. Dixon, "Bounds on deep neural network partial derivatives with respect to parameters," *arXiv preprint arXiv:2503.21007*, 2025.

[42] P. Ioannou and J. Sun, *Robust Adaptive Control*. Prentice Hall, 1996.

[43] R. Ortega, J. G. Romero, and S. Aranovskiy, "A new least squares parameter estimator for nonlinear regression equations with relaxed excitation conditions and forgetting factor," *Syst. Control Lett.*, vol. 169, p. 105377, 2022.

[44] H. K. Khalil, *Nonlinear Systems*. Prentice Hall, 3 ed., 2002.

[45] J. J. Slotine and W. Li, "Composite adaptive control of robot manipulators," *Automatica*, vol. 25, pp. 509–519, July 1989.

[46] E. A. Coddington and N. Levinson, *Theory of Ordinary Differential Equations*. McGraw-Hill, 1955.



Rebecca G. Hart is a Ph.D. candidate in Mechanical Engineering at the University of Florida, advised by Dr. Warren Dixon. She earned her Bachelor of Science in Mechanical Engineering from North Carolina State University in 2022 and her M.S. from the University of Florida in 2023. She is a recipient of the NSF Graduate Research Fellowship. Her research interests include Lyapunov-based control techniques, deep learning methods, and physics-informed learning.



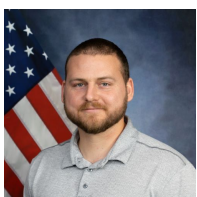
Prof. Warren Dixon received his Ph.D. in 2000 from the Department of Electrical and Computer Engineering from Clemson University. He worked as a research staff member and Eugene P. Wigner Fellow at Oak Ridge National Laboratory (ORNL) until 2004, when he joined the University of Florida in the Mechanical and Aerospace Engineering Department. His main research interest has been the development and application of Lyapunov-based control techniques for uncertain nonlinear systems. His work has been recognized

by the 2019 IEEE Control Systems Technology Award, (2017-2018 & 2012-2013) University of Florida College of Engineering Doctoral Dissertation Mentoring Award, 2015 & 2009 American Automatic Control Council (AACC) O. Hugo Schuck (Best Paper) Award, the 2013 Fred Ellersick Award for Best Overall MILCOM Paper, the 2011 American Society of Mechanical Engineers (ASME) Dynamics Systems and Control Division Outstanding Young Investigator Award, the 2006 IEEE Robotics and Automation Society (RAS) Early Academic Career Award, an NSF CAREER Award (2006-2011), the 2004 Department of Energy Outstanding Mentor Award, and the 2001 ORNL Early Career Award for Engineering Achievement. He is an ASME Fellow (2016) and IEEE Fellow (2016), was an IEEE Control Systems Society (CSS) Distinguished Lecturer (2013-2018), served as the Director of Operations for the Executive Committee of the IEEE CSS Board of Governors (BOG) (2012-2015), and served as an elected member of the IEEE CSS BOG (2019-2020). His technical contributions and service to the IEEE CSS were recognized by the IEEE CSS Distinguished Member Award (2020). He was awarded the Air Force Commander's Public Service Award (2016) for his contributions to the U.S. Air Force Science Advisory Board. He is currently or formerly an associate editor for ASME Journal of Dynamic Systems, Measurement and Control, Automatica, IEEE Control Systems, IEEE Transactions on Systems Man and Cybernetics: Part B Cybernetics, and the International Journal of Robust and Nonlinear Control.



Omkar Sudhir Patil received his Bachelor of Technology (B.Tech.) degree in production and industrial engineering from Indian Institute of Technology (IIT) Delhi in 2018, where he was honored with the BOSS award for his outstanding bachelor's thesis project. In 2019, he joined the Nonlinear Controls and Robotics (NCR) Laboratory at the University of Florida under the guidance of Dr. Warren Dixon to pursue his doctoral studies. Omkar received his Master of Science (M.S.) degree in mechanical engineering in 2022 and Ph.D.

in mechanical engineering in 2023 from the University of Florida. During his Ph.D. studies, he was awarded the Graduate Student Research Award for outstanding research. In 2023, he started working as a postdoctoral research associate at NCR Laboratory, University of Florida. His research focuses on the development and application of innovative Lyapunov-based nonlinear, robust, and adaptive control techniques.



Zachary I. Bell received his Ph.D. from the University of Florida in 2019 and is a researcher for the Air Force Research Lab. His research focuses on cooperative guidance and control, computer vision, adaptive control, and reinforcement learning.